OPTICAL COMMUNICATION

The use of light as a signaling medium is not a recent development; communicating using light is a very basic concept. Visual communication systems have been used for centuries, including smoke signals, beacon fires, and semaphores. Even more modern concepts, such as optical communications for telephone systems, are far from being new ideas; a century ago, in 1880, Alexander Graham Bell developed the Photophone, capable of transmitting speech over several hundred meters using visible light beams; by comparison, Marconi demonstrated wireless radio for the first time in 1895. Although Bell's early system was crude by today's standards and proved to be impractical, it nevertheless set the stage for exploration of optical frequencies for communications (1,2). Over the years, progress in fiber optics has been the result of an interdisciplinary collaboration involving electrical engineers, physicists, materials scientists, and others (this method of development has also characterized semiconductor electronics). As a result, many of the key enabling technologies such as semiconductor lasers, low loss optical fibers, and integrated electronics were developed approximately at the same time. We can trace the development of modern optical fiber communications to a combination of incremental innovations in the existing art and scientific breakthroughs (such as the invention of the laser), which led to entirely new technologies.

As communication engineers sought to investigate higher and higher frequencies for transmission, eventually leading to microwave systems in the early 1940s, speculation on the use of optical communications began in the years following World War II. This background of theory was put to use when the laser was first described by Townes and Schawlow in 1958, and subsequently demonstrated for the first time by

Maiman in 1960. Thus began a prolific period of development in the technology that would make optical communications practical. Following a proposal in 1966 by Kao (a British engineer with the Standard Telecommunications Laboratory) that loss in glass fibers could be significantly reduced to very low levels, Corning Glass Works proceeded to develop the first practical optical fiber (with loss below 20 dB/km) in 1970. Advances in the following years led to losses of well below 1 dB/km, at about the same time that semiconductor lasers became available that were capable of continuous operation at room temperature. By the mid-1970s demonstrations of optical fiber communications systems was well under way, which ultimately led to the proliferation of fiber systems in the telecommunications infrastructure.

Initially, the predominant use of optical fiber has been as a replacement for point-to-point electrical wiring, except at much higher data rates and longer distances. While this represents an important advance in communication technology, it is far from realizing the inherent potential of optical communication systems. Just as electrical communications has evolved from the inception of point-to-point telegraph systems to modern networks which combine voice, data, video and other types of multimedia, optical communication has been growing from a simple drop-in replacement for copper wire to the development of new types of communication designed specifically to take advantage of optical interconnects.

INTRODUCTION

It is important to realize that while optical communication may appear to be simply an extension of electronic communications using copper wire, the two are fundamentally very different phenomena. While it can be useful to think of light traveling in a fiber in the same way that electricity does in a wire, this analogy can be misleading. Light is an electromagnetic wave and the optical fiber is a waveguide; the fundamental principles of optical communications are all based on guided waves, rather than voltage and current potentials. Even fairly simple concepts such as joining two fibers together (coupling) is done very differently from splicing a pair of electrical wires. While electronic and optical communications are closely related, they employ different principles and apply them in different ways.

The basic components of an optical communication system are shown in the block diagram of Fig. 1; they consist of the following:

An electrical data stream to be transmitted from the sender to the receiver.

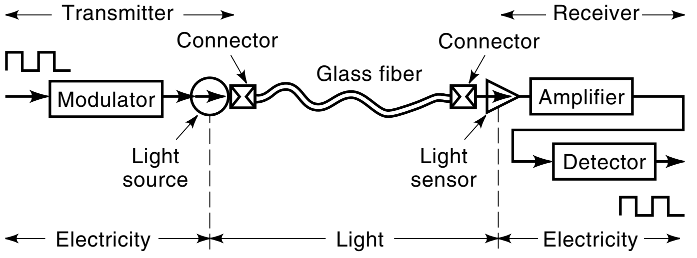

Figure 1. Block diagram, basic optical communication system.

An optical source (such as a laser or light emitting diode) that is modulated by the electrical data and couples the modulated light into an optical fiber.

The optical fiber cable, which can be of several different types. Signals experience dispersion and lose their strength as they travel along the fiber. The fiber typically includes at least one optical connection at either end to couple light into and out of the fiber, possibly using additional lenses or optical elements, as well as couplers, splices, splitters, or other components along the path.

An optical receiver (such as a photodiode), which converts the optical signal back into electrical form. This step may be followed by additional electronics that amplify the signal, decode the transitions of individual data bits and their relative timing, and reconstructs an approximation of the original data stream presented to the sender.

There are many applications for optical communication links in telecommunications, data communications, and analog systems. Telecommunication applications consist primarily of voice traffic, although increasingly multimedia applications are running over the voice network. Datacom systems provide interconnections between computer equipment and have somewhat different requirements; they typically use shorter distances than telecom links, operate at lower bit error rates because the consequences of a single bit error are more severe, must maintain international class 1 (inherently safe) optical power levels at all times, and must be robust enough to withstand frequent handling. Telecom links, by contrast, are handled only by trained professionals, but because they are much longer they also encounter concerns with outdoor cable (either buried underground or suspended from towers) or undersea cable. Analog communication systems have been reserved for military applications, although recent developments in cable television distribution may take advantage of this technology. While digital systems often use direct (incoherent) detection schemes, some analog systems employ coherent detection. In this case, the received optical signal is combined with a local oscillator in the form of an unmodulated beam of light derived from the same source; mixing these two signals allows the detection of the modulated information in the same way that analog radio frequency (RF) communication systems operate. Because of the difficulty in deriving a suitable reference light beam, this technique is typically restricted to military applications and related areas.

Optical sources, including semiconductor lasers, light emitting diodes (LEDs), and vertical cavity surface emitting lasers (VCSELs), as well as semiconductor optical detectors, including positive–intrinsic–negative (p–i–n) and avalanche photodiodes are treated in detail elsewhere in the encyclopedia. The manufacturing of optical fiber and cables is treated in detail elsewhere, and industry standards are available for fiber optic testing, installation of fiber, fire safety requirements for optical cables, and laser safety for optical transmitters (1–10). The fundamentals of optical fiber, optical coupling, and link design will be treated in more detail later. Optical communication has been widely adopted because it offers many well-known advantages such as the following:

1. *Information Capacity.* Optical fibers offer inherently higher potential data transmission rates than electrical

wires. The theoretical bandwidth of a single-mode optical fiber is approximately 25 THz or enough capacity to carry all of the world's telephone traffic at peak usage on one pair of fibers. While it is not possible to exploit this full potential today, systems operating in the hundreds-of-gigabits range have been demonstrated in laboratory experiments. Existing electronics cannot be operated at such high speeds; however, fibers offer the ability to multiplex different optical wavelengths on a single fiber without interference. In this way, many high-speed data streams can be combined on a single fiber to approach data rates far exceeding conventional copper wiring. Furthermore, optical fibers offer a larger bandwidth-distance product, which is an important measure of the usefulness of a communication channel. A single copper wire may be able to carry gigabit data rates, but only over distances of a few meters; in contrast, optical fiber offers bandwidth-distance products in the range of terabits over hundreds of kilometers. Fiber optic technology is still in its infancy in this regard, and future systems are expected to take fuller advantage of this capacity. A related advantage of optical fiber is the ability to enhance the capacity of existing fiber links as new technology becomes available simply by changing the equipment at either end of the link; it is not required to change the fiber itself.

2. *Distance Between Signal Regenerators.* As noted above, the bandwidth-distance product of optical fiber enables high-fidelity transmission over long distances. As a signal travels along a communication link, it decreases in strength (attenuation) and is corrupted by various types of noise. Data pulses also tend to spread out as they propagate (dispersion) and begin to interfere with adjacent pulses. After some distance, the signal must be strengthened and its noise removed by using a repeater or amplifier; timing information may also be recovered by retiming or regenerating the signal. Because optical fiber offers a higher bandwidth-distance product, signals at a given data rate will travel farther in optical fiber before requiring regeneration. For example, commercial phone lines require repeaters spaced about every 12 km; optical links have increased this distance to around 40 km, and some recently installed systems (1997) extend the unrepeated distance up to 120 km or more.
3. *Immunity to Electromagnetic Interference.* It is an obvious but very important point that there are no electrical components along a fiber link, except for the electronics at either end or at the repeaters. This means that the transmission medium (glass fibers) can neither pick up nor create electrical interference. There are very few things which can interfere with or distort an optical signal traveling along a fiber; this is one reason why optical communication offers such high-fidelity transmission. This means that optical fiber can be used in locations where electrical cable would not be able to function, such as near a noise source such as an electrical motor or in a cable duct next to heavy-duty power lines. Since there is no danger of electrocution from an optical cable, it may be routed near water or other hazards; the optical fiber is very safe, because it isolates the transmission medium from high voltages at either end of the link. Outdoor optical cable does not require special lightning protection. In a network environment, there is much greater flexibility in selecting a route for optical fiber. Electrical communication systems are also subject to ground loops, or small voltage potentials between points in the link which should be a common ground; this problem is particularly acute if electrical cables are grounded at both ends of a long link. Of course, this problem is not present when using optical fiber, which acts to electrically isolate equipment on both ends of the link.
4. *Improved Security.* Because optical fiber is nonconductive, it does not radiate electromagnetic fields; metallic cables require additional shielding to achieve similar effects. It is possible to eavesdrop by tapping a fiber optic cable, but it is very difficult to do and the additional loss caused by the tap is relatively easy to detect and locate. Tapping an optical fiber will generally require interrupting the link while the tap is inserted, and there are few access points where an intruder can gain the intimate access to a fiber cable necessary to insert a tap. Placement of active taps that insert false signals onto the optical link is even more difficult. Thus, optical fiber offers greater security for data transmission.
5. *Weight, Size, and Material Cost.* For the same transmission capacity, the material cost for optical fiber is significantly less than for copper cable, and offers a significant reduction in both cable diameter and cable weight. Optical cable is much more flexible due to its small size, and can be routed around tight bends or through small holes more easily. This also means that the cost of installing fiber cable is significantly reduced.

We must also point out that any communication technology has limitations and weaknesses; some of the disadvantages of optical fiber include the following:

1. *More Complex Terminations.* Multimode fibers are about the same diameter as a human hair; single mode fibers are even smaller. Because optical fiber is a waveguide, two fibers cannot simply be spliced in the same way as electrical wires. Instead, the fiber ends must be aligned with each other, then joined by melting the glass (fusion splicing). Although splicing technology is fairly well developed, making durable low-loss splices remains a skilled task that requires precision equipment. It is particularly difficult to do under extremes of temperature or in tight physical locations. Pluggable optical connectors have been developed with good reliability and low loss, although single-mode connections remain more difficult than multimode connections and contamination from even small amounts of dirt can obscure the fiber endface if connectors are not properly cleaned before use. The difficulty of aligning fibers with optical sources or detectors remains one of the most important factors contributing to the high cost of optical transceivers as compared with electrical transceivers.
2. *Bending Loss.* As light travels along a fiber waveguide, the fiber's composition is designed to bend light back toward the fiber core and away from the outer cladding.

This guiding mechanism allows light to remain confined within the fiber when the fiber is bent; however, if the bending radius becomes too great, light will escape from the fiber core and the signal strength will greatly diminish. For this reason, optical fibers cannot bend too sharply; the allowed bend radius varies with specific cables because it depends on the difference in refractive index between the core and cladding. As we will see, there is a tradeoff involved; for many reasons we would like to keep this difference as small as possible, yet the smaller the index difference, the larger the bend radius limit.

3. *Susceptibility to Different Noise Sources.* Some types of optical fibers function as a waveguide with many different modes supported at the same time. If light is not coupled into the fiber in the proper way, or if there are flaws in the fiber, then some modes will propagate at greater velocities than others. This intermodal delay can cause severe limits in the performance of optical communication systems, and it is one reason why optical transceiver designs are different for single-mode and multimode fiber. The glass used in optical fiber is typically doped with small concentrations of impurities to improve the optical transmission properties; this makes optical fiber susceptible to ionizing (gamma) radiation. Similarly to high-energy X rays, large amounts of this type of radiation can cause glass to become opaque to the optical signal wavelengths. In some types of glass, gamma radiation can also cause spontaneous emission of light, which interferes with the desired signal. Optical cable placed in environments such as nuclear power plants, space satellites, or medical centers must allow for this effect; when optical fiber is buried or placed undersea, the long-term cumulative effects of background radiation may limit the fiber's effective lifetime. Very high voltage electrical fields (above 30,000 V) can affect glass in the same way as gamma radiation; this presents a concern for routing optical cable along high-voltage power lines. Finally, although optical cables are surprisingly rugged, they must be carefully shielded in outdoor environments where insects and rodents (particularly gophers) can attack the cable. There is actually a standardized test for outdoor cables, conducted by approved wildlife organizations, which involves placing cables in a gopher enclosure for a specified length of time and observing the resulting damage.

FUNDAMENTALS OF OPTICAL FIBER

To understand how light propagates in an optical fiber, we must first introduce the mathematical expressions for light wave propagation. Light is most accurately described as a vector electromagnetic wave (1–10), in the same manner as any other component of the electromagnetic spectrum (Fig. 2). This is the only satisfactory way to describe light propagation in a singlemode fiber; however, this level of complexity is often not required for describing many important properties of fiber optics.

A good approximation to describing optical coupling can be obtained from geometric optics by considering light rays emanating from an optical source and impinging on the end-

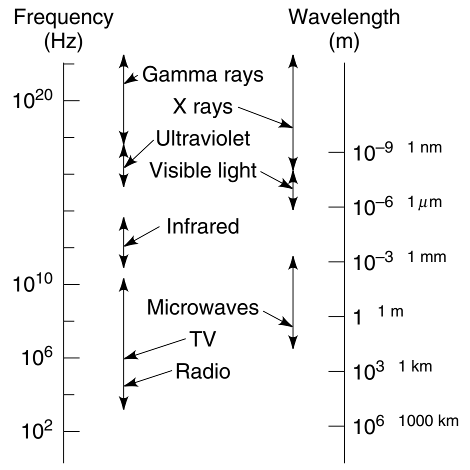

Figure 2. The electromagnetic spectrum.

face of a glass fiber (Fig. 3). We know from Snell's Law (1) that incoming light rays will be refracted when they strike the glass core at an angle; once the rays enter the fiber, they undergo refraction again at the interface between the fiber core and the outside environment. To make the fiber function as a waveguide, the core is surrounded by another layer of material called the cladding. The glass fiber acts as a waveguide if there is a difference in refractive index between the fiber core and cladding materials. If the core has a higher refractive index than the cladding, light rays entering the fiber core at the proper angle are continuously refracted away from the core-cladding interface and continue to propagate along the fiber. This occurs only for light entering the fiber core with an acceptance cone defined by the angle θ in Fig. 3. It is conventional to describe the amount of light that can be coupled into a fiber in terms of the numerical aperture (NA), which is easily derived from Snell's Law as

$$\mathrm{NA} = n_1 \sin\theta \tag{1}$$

where n_1 is the refractive index of the media outside the fiber. For air, $n_1 = 1$ and the NA is simply defined as the sin of the largest angle contained within the acceptance cone. If the refractive index of the fiber core is n_2, then we can also redefine NA in terms of the dimensionless parameter Δ, which is given by

$$\Delta = n_1 - \frac{n_2}{n_2} \tag{2}$$

so that we have

$$\mathrm{NA} = n_1 \sqrt{2\Delta} \tag{3}$$

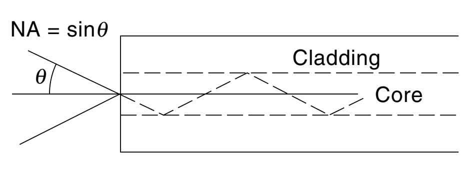

Figure 3. Definition of numerical aperture. Reprinted from Ref. 3, courtesy of Academic Press.

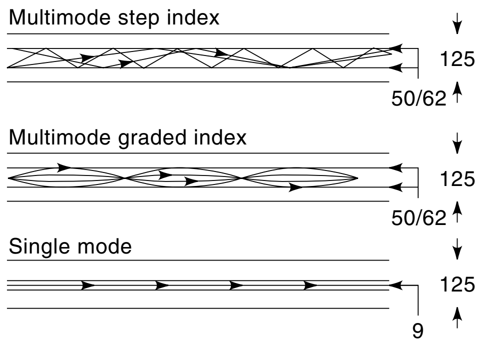

Figure 4. Definition of modes in an optical fiber. Ray paths are straight in step-index fiber and curved in graded index fiber due to the focusing properties of the graded index fiber core.

Consider many rays entering the fiber at various angles within the NA; all the rays propagate along the fiber, but at different angles (Fig. 4). Each ray path may be thought of as a mode of propagation; if the fiber core is large, many ray paths, or modes, are possible. This is known as a multimode optical fiber. Conceptually, if we reduce the size of the fiber core enough we reach a point where only one ray path, or mode, is bound within the fiber and all others are not guided. This is known as a single-mode fiber. We discuss the two different fiber types in more detail later; for now, note that the typical multimode fiber has a core diameter of approximately 50 μm to 62.5 μm, whereas a single-mode fiber has a core diameter of approximately 10 μm. Numerical aperture is a frequently quoted specification of optical fiber; for multimode fiber NA is typically between 0.2 and 0.3, while for single-mode fibers it is around 0.1. In addition to being a measure of the fiber's ability to collect light, NA is also a good measure of the light-guiding properties of the fiber. Larger NA corresponds to more modes and greater fiber dispersion. Larger NA also means that the fiber can undergo tighter bends (smaller bend radius) before bending loss becomes a problem. Furthermore, in single-mode fiber, higher NA means a higher contrast in refractive index between the core and cladding; this is often due to higher dopant concentrations in the cladding material. This doping increases the attenuation of the fiber; since a large portion of the light in single-mode fibers travels in the cladding, there will often be higher attenuation in single-mode fiber with larger NA.

The ray model for light propagation may lead us to believe that there are an infinity of possible paths for light rays to follow within the fiber, provided they are launched within the NA. However, this is not actually the case; light rays are drawn perpendicular to the optical wavefront, and are valid only for plane waves in which the diameter of the light beam is much larger than the wavelength. To fully understand light propagation within a fiber, we must return to the wave description of light. We assume a harmonically time-varying wave propagating in the z direction of Fig. 5 with phase constant β; the electric field can be expressed as

$$E = E_0(x, y)\cos(\omega t - \beta z) \tag{4}$$

or in phasor form, where the real part of the right-hand side is assumed,

$$E = E_0(x, y)e^{j(\omega t - \beta z)} \tag{5}$$

where E_0 is the peak amplitude, ω is the radian frequency, which is equal to $2\pi f$, f is the frequency in hertz, and β is the propagation constant defined by

$$\beta = 2\pi/\lambda = \omega/v \tag{6}$$

where v is the propagation velocity, or phase velocity, defined by

$$v = c/n \tag{7}$$

c is the speed of light, and n is the refractive index.

Note that the phase velocity describes the speed of the wavefront as it propagates along the fiber; this is slightly different than the group velocity, which describes the propagation of information such as a modulated wave packet along the fiber and is given by

$$v_g = d\omega/d\beta \tag{8}$$

If there is no dispersion in the medium then group velocity and phase velocity are the same; otherwise, phase velocity is slightly greater.

Since light is an electromagnetic wave, it is governed by Maxwell's equations (1); starting from these fundamental expressions, it is possible to derive the wave equation that describes propagation of the electric and magnetic fields in the z direction defined in Fig. 5. The wave equation for the longitudinal electric field component in the z direction is given by

$$\Lambda_t^2 E_z(x, y) + \beta_t^2 E_z(x, y) = 0 \tag{9}$$

where we have introduced the transverse Laplacian notation:

$$\Lambda_t^2 = \frac{d^2}{dx^2} + \frac{d^2}{dy^2} \tag{10}$$

and the transverse phase constant

$$\beta_t^2 = (2\pi n/\lambda)^2 - \beta^2 \tag{11}$$

When light is confined in space, boundary conditions imposed on the light restrict the phase constant to a limited number of values. Each possible phase constant represents a mode; thus, when light is confined within a fiber it can propagate only in a limited number of ways. Under ideal conditions, all

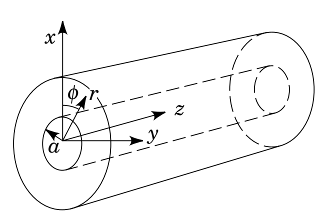

Figure 5. Typical optical fiber geometry. Reprinted from Ref. 3, courtesy of Academic Press.

of the propagating modes within a fiber are orthogonal, and there is no power transfer between modes or interference between one mode and another. In practice this often does not hold true, as we see in the discussion of link budgets. In almost all practical fibers, the refractive index difference between the core and cladding is small and the modes are called *weakly guided;* some modes enter the cladding, either due to the launch conditions or as a result of bends in the fiber. Still others called *leaky modes* satisfy the marginal case between being bound and being a cladding mode; these modes propagate for some distance before being lost from the core and cladding; in a short link, however, they may reach the optical receiver and create excess dispersion because their group velocities are much slower than the bound modes. Some link designers incorporate several tight bends in the fiber, intended to pass all bound modes and eliminate leaky ones; this practice is called mode stripping.

To find how many modes can propagate in a fiber, their phase constants, and their spatial profile, we must solve the wave equation for a specific fiber geometry. This is often done by transforming the wave equation into cylindrical coordinates to accommodate the geometry of a glass fiber. The solution depends on the refractive index profile of the fiber. The simplest case is a step index fiber (shown in Fig. 6), for which there is an abrupt transition of the refractive index at the core/cladding boundary. For step index fibers, a complete set of analytical solutions to the wave equation can be given; the solutions can be grouped into different types of modes, known as transverse electric (TE), transverse magnetic (TM), and hybrid modes. In practice the refractive index difference between core and cladding is very small, only approximately 0.005, so most of these modes are degenerate and it is sufficient to use a single notation for all types, calling them lateral polarization (LP_{lm}) modes (where the subscripts l and m refer to the number of radial and azimuthal zeros for a particular mode). To determine if a given LP mode will propagate, it is very useful to define the normalized frequency, or V number, of the fiber,

$$V = ka\sqrt{n_1^2 - n_2^2} \tag{12}$$

and the normalized propagation constant for a particular mode, b, give by

$$b = \frac{(\beta^2/k^2) - n_2^2}{n_1^2 - n_2^2} \tag{13}$$

Rather than use the formal definition for b given above, for LP modes, Gloge et al. (11) has derived a series of analytical formulas to determine b for different modes to a very good approximation. Using these expressions, we can plot $b(V)$ as shown in Fig. 7. It can be seen that for guided modes, b varies between 0 and 1; the wavelength for which $b = 0$ is called the cut-off wavelength,

$$b(V) = 0 \rightarrow \lambda_{co} = (2\pi/V)a\,n_1\sqrt{2\Delta} \tag{14}$$

where a is the core radius. Therefore, a mode cannot propagate in the fiber if its wavelength is longer than the cut-off wavelength. Cut-off values for the V number have been tabulated (11). It is also possible to determine the spatial intensity distributions of these modes; to a very close approximation,

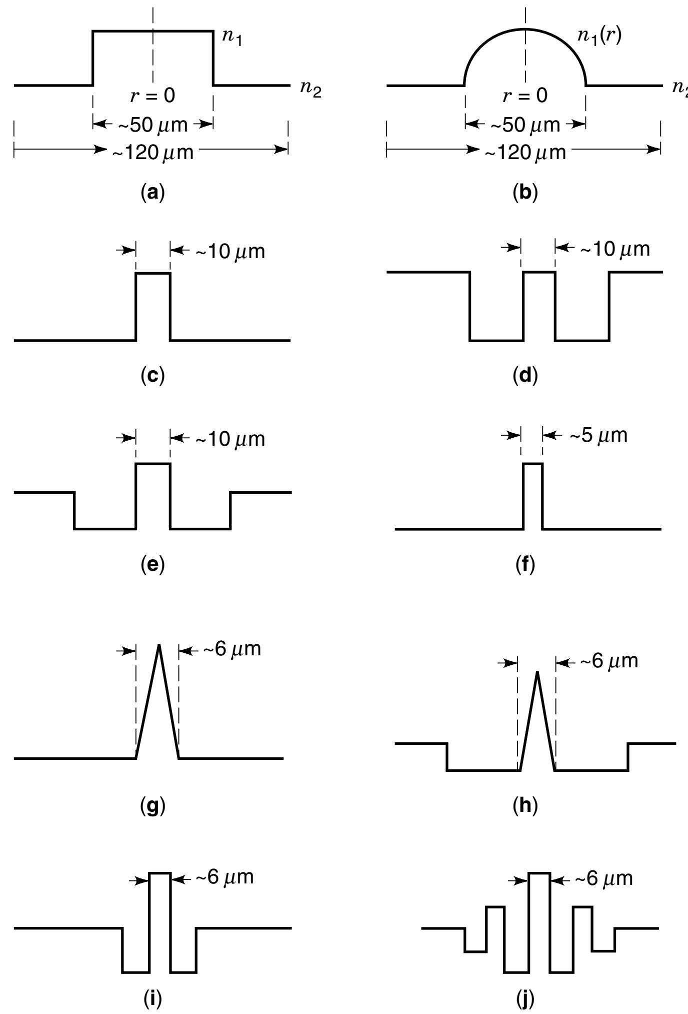

Figure 6. Refractive index profiles of (a) step-index multimode fibers, (b) graded index multimode fibers, (c) match cladding singlemode fibers, (d,e) depressed cladding single-mode fibers, (f–h) dispersion shifted fibers, and (i,j) dispersion flattened fibers. Reprinted from Ref. 3, courtesy of Academic Press.

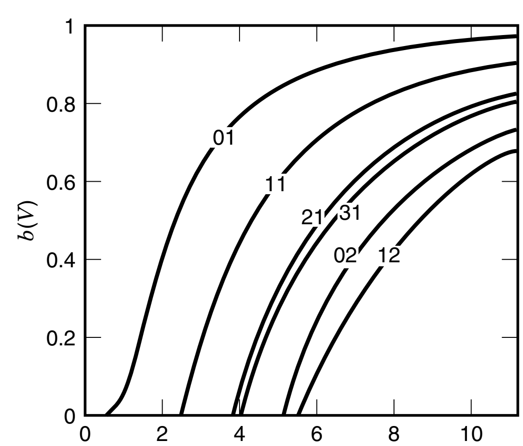

Figure 7. Cutoff frequencies for the lowest order LP modes; $b(V)$ is the normalized propagation constant as a function of V number. Reprinted from Ref. 3, courtesy of Academic Press.

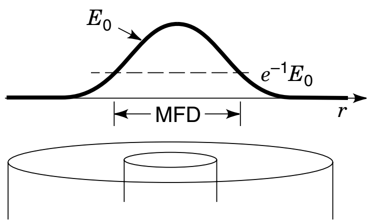

Figure 8. Definition of mode field diameter in an optical fiber. Reprinted from Ref. 3, courtesy of Academic Press.

the fundamental mode can be described as a Gaussian function,

$$E(r) = E_0 \exp[-(r/w)^2] \tag{15}$$

where E_0 is the amplitude and $2w$ is called the mode field diameter (MFD). The MFD is another important parameter; it represents the optical spot size that carries most of the optical power (mathematically, the diameter of the spot for which the power has decreased by e^{-2} or the amplitude has decreased by e^{-1}). As illustrated in Fig. 8, the MFD is not necessarily the same dimension as the fiber core; it is larger than the core of a single-mode fiber, thus much of the optical power in a single-mode fiber is carried by the cladding. The MFD is much smaller than the core diameter of a typical multimode fiber. For wavelengths between 0.8 and 2 times the cutoff wavelength, the optimum MFD (12) is given by

$$\frac{w}{a} = 0.65 + 1.69V^{-3/2} + 2.87V^{-6} \tag{16}$$

The radial distribution for higher order modes can be obtained using Bessel functions (13).

The preceding discussion is valid only for step index fibers; in practice, the refractive index of the core material is usually graded as shown in Fig. 6. This causes different modes to propagate with similar velocities. The various graded index profiles are described by the expression

$$\begin{aligned} n^2(r) &= n_1^2(1 - 2\Delta(r/a)^q) \quad \text{for } 0 \le r \le a \\ n^2(r) &= n_1^2(1 - 2\Delta) = n_2^2 \quad \text{for } r \ge a \end{aligned} \tag{17}$$

where q is called the profile exponent. The optimum profile for minimum dispersion is given for q slightly less than 2. For multimode fibers, the total number of modes, N, which can propagate is given by

$$N = \tfrac{1}{2}V^2 \frac{q}{q+2} \tag{18}$$

This expression is only valid for large V numbers; for a step index fiber q is infinite and

$$N = V^2/2 \tag{19}$$

The different ray paths possible in multimode fiber can be calculated from geometric optics (1). A more accurate approach is to solve the wave equation using the so-called WKB approximation (13,14). The phase constants for different modes can be shown to obey the following relationship:

$$\beta_m = n\,k\sqrt{1 - 2\Delta(m/n)^{q/q+2}} \quad \text{for } m = 1, 2, \ldots, N \tag{20}$$

Optical Coupling

Some typical properties of optical fibers are shown in Table 1. For an incoherent light source such as a light emitting diode (LED), the total power accepted by the fiber, P, is given by

$$P = \pi BA(\text{NA})^2 \tag{21}$$

where B is the LED's radiance in units of watts per area and steradian and A is the cross-sectional area of the fiber. Given the total power accepted by the fiber, the coupling efficiency may be defined as

$$\eta = P_{\text{lm}}/P_{\text{in}} \tag{22}$$

where P_{in} is the power launched into the fiber and P_{lm} is the power accepted by the LP_{lm} mode. For optical link budget η analysis, it is more convenient to express coupling loss in decibels,

$$\alpha = 10 \log \eta \tag{23}$$

For coherent light sources, such as lasers, which can be approximated by a Gaussian beam, the coupling efficiency for the LP_{01} mode in single-mode fiber may be calculated analytically (12,15)

$$\eta = \frac{4D}{B} \exp\left(-\frac{AC}{B}\right) \tag{24}$$

where

$$A = \frac{(2\pi\, n\, s_1/\lambda)^2}{2} \tag{25}$$

$$B = G^2 + (D+1)^2 \tag{26}$$

$$C = (D+1)F^2 + 2DFG\sin\theta + D(G^2 + D + 1)\sin^2\theta \tag{27}$$

$$D = \left(\frac{s_2}{s_1}\right)^2 \tag{28}$$

$$F = \frac{2\Delta}{2\pi\, n\, s_1^2/\lambda} \tag{29}$$

$$G = \frac{2\Delta Z}{2\pi\, n\, s_1^2/\lambda} \tag{30}$$

Table 1. Typical Properties of Single-mode Optical Fiber Compliant with CCITT Recommendation G.652a

Parameters	Specifications
Cladding diameter	125 μm
Mode field diameter	9–10 μm
Cutoff wavelength λ_{co}	1100–1280 nm
1550 nm bend loss	≤1 dB for 100 turns of 7.5 cm diameter
Dispersion	≤3.5 ps/nm · km between 1285 and 1330 nm
	≤6 ps/nm · km between 1270 and 1340 nm
	≤20 ps/nm · km at 1550 nm
Dispersion slope	≤0.095 ps/nm^2 · km

Reprinted from Ref. 3, courtesy of Academic Press.

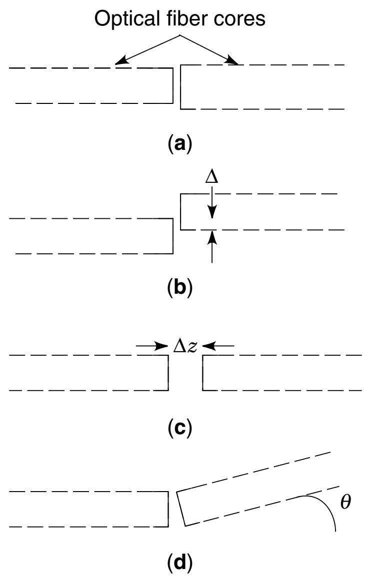

Figure 9. Different coupling cases for optical fiber cores. (a) Mismatch in core size and mode field diameter (spot size); (b) transverse offset; (c) lack of physical contact or lateral offset; (d) angular misalignment. Reprinted from Ref. 3, courtesy of Academic Press.

where ΔZ is the separation distance between source and fiber, Δ is the lateral displacement, θ is the angular displacement, and s_1 and s_2 are the mode field radii or spot sizes of the source field and fiber field, respectively. This expression takes into account four different coupling cases, shown in Fig. 9; if only one condition is present at a time, the expression simplifies as follows:

Spot size mismatch (s_1 not equal to s_2):

$$\eta = \left(\frac{2s_1s_2}{s_1^2 + s_2^2}\right)^2 \tag{31}$$

Transverse offset, Δ

$$\eta = \exp[-(\Delta/s_2)^2] \tag{32}$$

Longitudinal offset ΔZ

$$\eta = \frac{1}{1 + (\Delta Z/2Z_0)^2} \tag{33}$$

Angular misalignment, θ

$$\eta = \exp[-(\theta/\theta_0)^2] \tag{34}$$

All of these expressions must be modified if a lens system is used to couple light into a fiber; they must also be corrected for reflection losses at the fiber endface (16). These expressions are important in the design of optical connectors and splices to minimize loss in the optical link budget.

Both mechanical and optical characteristics must be considered in the design of optical interfaces between fibers and active devices, or between a pair of fibers. It is desirable to control the launch conditions from a source into a fiber such that at least 70% of the light is captured in 70% of the fiber's NA, a so-called equilibrium mode launch. Typically, the optical fiber is threaded into a ceramic ferrule, which in turn is part of a connector assembly. The ferrule is then inserted into bores that house the optical transmitter and receiver. Two kinds of bores are available, solid and split sleeve. A solid sleeve is a cylinder of rigid ceramic material, as shown in Fig. 10, whereas a split sleeve is made of plastic or other flexible material and is designed to enlarge slightly to accommodate the ferrule. Split sleeves are most commonly used in fiber-to-fiber couplers, whereas solid bores are often found in optical transceivers. When inserting a ferrule into an optical transceiver, the position of the optical axis relative to the mechanical axis of the bore is known as the beam centrality (BC). The corresponding misalignment between the centerlines of the ferrule and the fiber, due to imperfect ferrule manufacturing, is known as the ferrule–core eccentricity (FCE). It is desirable to have both BC and FCE equal to zero for optimal alignment. Even when this is the case, the laser beam may still possess some small tilt, known as the pointing angle, that adversely affects coupling. Furthermore, the ferrule endface may not be polished exactly flat, or may be deliberately polished at a 5° to 10° angle to minimize reflections.

Optical sources and detectors are often packaged together to form transceivers capable of bidirectional communication over a pair of optical fibers. Such transceivers accept a duplex optical connector, which compounds the alignment problems further. The axial misalignment of the entire optical subassembly and bore from its desired position in the transceiver is called subassembly misalignment (SAM). To partially compensate for alignment errors, most optical connectors are designed with some amount of lateral movement or float, which enables the ferrule to be moved slightly within the connector assembly when it is plugged into a transceiver. Other characteristics of the transceiver that affect optical coupling are the connector body dimensions and transceiver receptacle dimensions. Poor control of the mating tolerances can lead to two basic problems. First, the same connector plugged into the same transceiver may exhibit excessive variation in the launched power; this is known as plug repeatability. Second,

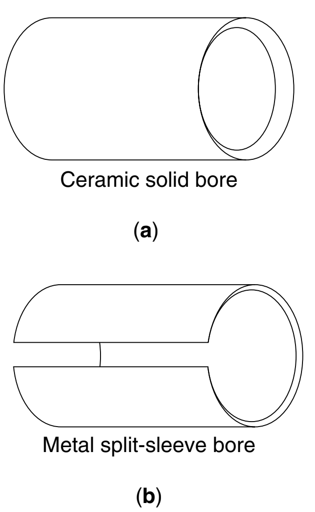

Figure 10. Solid and split-sleeve bores. (a) Ceramic solid bore. (b) Metal split-sleeve bore. Reprinted from Ref. 3, courtesy of Academic Press.

Table 2. Typical Values Affecting Optical Metrology

		Influence on CPR	
Element	Typical Value	Solid Bore	Split Sleeve
BD	2.5010–2.5025 mm	X	
BC	3.3 ± 2.0 μm	XX	XX
PA	<3°	XX	XX
SBS	5–20 μm	XX	XX
FD	2.4992–2.5000 mm	X	
FCE	<1.6 μm (0.7 μm)	X	X
EFA	0.1°–0.2°	X	X
FBS	9.5 ± 0.5 μm (SM only)	X	X
SAM	spec. ± 0.34 mm		X
FF	spec. ± 0.34 mm		X
SD	spec. ± 0.125 mm		X
CD	spec. ± 0.125 mm		X

Reprinted from Ref. 4, courtesy of Academic Press.

when multiple connectors are mated with the same transceiver the difference between the highest and lowest coupled power levels is known as the cross-plug range; it is desirable to keep this as low as possible. When designing the interface between an optical fiber and a light source, an important parameter is the coupled power range (CPR) or the allowable difference between minimum and maximum optical power levels. For example, the maximum power level may be determined by laser safety standards, while the minimum power is determined by the need to achieve a desired bit error rate when measured with a given receiver sensitivity. Establishing the CPR for a given application requires an understanding of the optical link budget, which is discussed in the following section. There are about a dozen key characteristics of the optical interface metrology that affect coupled power ratio; these are summarized in Table 2 along with typical values. For solid bore transceivers, only eight parameters have a significant effect on alignment; the first four parameters in Table 2 are related to the transceiver design and the second four are related to the connector design. The relative effect of each parameter on CPR is indicated by the number of X's shown; a blank column indicates no effect, one X indicates some effect, and two X's indicate a significant effect. When all the components of radial, axial, and angular misalignment are present together, they can interact in such a way that some parameters become even more critical in determining CPR. Analytic solutions for misalignments in the same plane are given by Nemoto and Makimoto (15,17); out-of-plane alignments are more difficult to analyze. Transceiver manufacturers typically employ some combination of active alignment (which involves alignment of a source and detector while both are operational) and passive alignment (which depends on the mechanical tolerances of the design) in different products.

LINK BUDGET

An optical transmitter is capable of launching a limited amount of optical power into the fiber; there is a limit to how weak a signal can be detected by the receiver in the presence of noise. Thus, a fundamental consideration is the optical link power budget, or the difference between the transmitted and received optical power levels. Some power is lost by connections, splices, and bulk attenuation in the fiber. There may also be optical power penalties due to dispersion, modal noise, or other effects in the fiber and electronics. The optical power levels define the signal-to-noise ratio at the receiver, Q; this is related to the bit error rate (BER) by the Gaussian integral

$$\mathrm{BER} = \frac{1}{\sqrt{2\pi}} \int_Q^\infty \exp\left(-\frac{Q^2}{2}\right) dQ \cong \frac{1}{Q\sqrt{2\pi}} \exp\left(-\frac{Q^2}{2}\right) \tag{35}$$

From Eq. (35), we see that a plot of BER and the received optical power yields a straight line on a semilog scale, as illustrated in Fig. 11. Nominally, the slope is approximately 1.8 dB/decade; deviations from a straight line may indicate the presence of nonlinear or non-Gaussian noise sources. Some effects, such as fiber attenuation, are linear noise sources; they can be overcome by increasing the received optical power, as seen from Fig. 11, subject to constraints on maximum optical power (laser safety) and the limits of receiver sensitivity. There are other types of noise sources, such as mode partition noise or relative intensity noise (RIN), which are independent of signal strength. When such noise is present, no amount of increase in transmitted signal strength will affect the BER; a noise floor is produced, as shown by curve B in Fig. 11. This type of noise can be a serious limitation on link performance. If we plot BER against receiver sensitivity for increasing optical power, we obtain a curve similar to Fig. 12 which shows that for very high power levels, the receiver will go into saturation. The characteristic bathtub-shaped curve illustrates a window of operation with both upper and lower limits on the received power. There may also be an upper limit on optical power because of eye safety considerations.

We can see from Fig. 11 that receiver sensitivity is specified at a given BER, which is often too low to measure directly in a reasonable amount of time (for example, a 200 Mbit/s link operating at a BER of 10^{-15} will only take one error every 57 days on average, and several hundred errors are recommended for a reasonable BER measurement). For practical

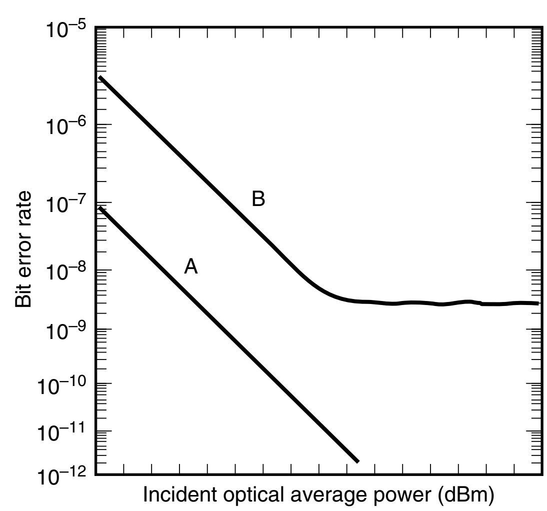

Figure 11. Bit error rate as a function of received optical power. Curve A shows typical performance, whereas curve B shows a BER floor. Reprinted from Ref. 3, courtesy of Academic Press.

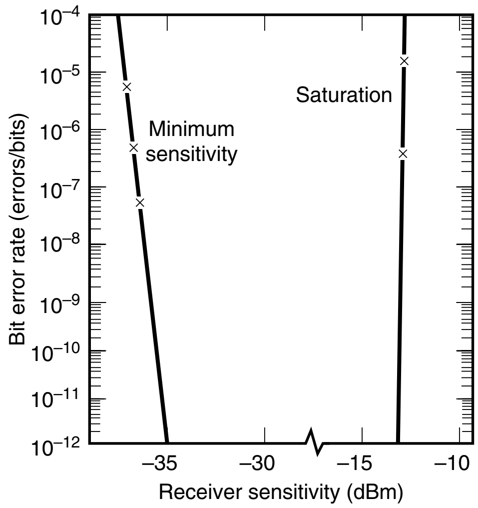

Figure 12. Bit error rate as a function of received optical power illustrating range of operation from minimum sensitivity to saturation. Reprinted from Ref. 3, courtesy of Academic Press.

reasons, the BER is typically measured at much higher error rates, where the data can be collected more quickly (such as 10^{-4} to 10^{-8}) and then extrapolated to find the sensitivity at low BER. This assumes the absence of nonlinear noise floors, as cautioned previously. The relationship between optical input power, in watts, and the BER, is the complimentary Gaussian error function

$$\mathrm{BER} = 1/2\,\mathrm{erfc}(P_{\mathrm{out}} - P_{\mathrm{signal}}/\mathrm{rms\ noise}) \tag{36}$$

where the error function is an open integral that cannot be solved directly. Several approximations have been developed for this integral, which can be developed into transformation functions that yield a linear least-squares fit to the data (1). The same curve-fitting equations can also be used to characterize the eye window performance of optical receivers. Clock position/phase and BER data are collected for each edge of the eye window; these data sets are then curve fitted with the above expressions to determine the clock position at the desired BER. The difference in the two resulting clock positions on either side of the window gives the clear eye opening (2–4).

In describing Figs. 11 and 12, we also have made some assumptions about the receiver circuit. Most data links are asynchronous and do not transmit a clock pulse along with the data; instead, a clock is extracted from the incoming data and used to retime the received datastream. We have made the assumption that the BER is measured with the clock at the center of the received data bit; ideally, this occurs when we compare the signal with a preset threshold to determine if a logical "1" or "0" was sent. When the clock is recovered from a receiver circuit such as a phase lock loop, there is always some uncertainty about the clock position; even if it is centered on the data bit, the relative clock position may drift over time. The region of the bit interval in the time domain where the BER is acceptable is called the eyewidth; if the clock timing is swept over the data bit using a delay generator, the BER will degrade near the edges of the eye window. Eyewidth measurements are an important parameter in link design, which is discussed further in the section on jitter and link budget modeling.

To design a proper optical data link, the contribution of different types of noise sources should be assessed when developing a link budget. There are two basic approaches to link budget modeling. One method is to design the link to operate at the desired BER when all the individual link components assume their worst-case performance. This conservative approach is desirable when very high performance is required, or when it is difficult or inconvenient to replace failing components near the end of their useful lifetimes. The resulting design has a high safety margin; in some cases, it may be overdesigned for the required level of performance. Because it is very unlikely that all the elements of the link will assume their worst-case performance at the same time, an alternative is to model the link budget statistically. For this method, distributions of transmitter power output, receiver sensitivity, and other parameters are either measured or estimated. They are then combined statistically using an approach such as the Monte Carlo method, in which many possible link combinations are simulated to generate an overall distribution of the available link optical power. A typical approach is the three-sigma design, in which the combined variations of all link components are not allowed to extend more than three standard deviations from the average performance target in either direction. The statistical approach results in greater design flexibility and generally increased distance compared with a worst-case model at the same BER.

Installation Loss

It is convenient to break down the link budget into two areas: installation loss and available power. Installation or DC loss refers to optical losses associated with the fiber cable plant, such as connector loss, splice loss, and bandwidth considerations. Available optical power is the difference between the transmitter output and receiver input powers, minus additional losses from optical noise sources on the link. With this approach, the installation loss budget may be treated statistically and the available power budget as worst case.

First, we consider the installation loss budget. Some of the important factors to be considered include the following: fiber cable loss (transmission loss), fiber attenuation as a function of wavelength, connector loss, and splice loss.

Transmission Loss. Transmission loss is perhaps the most important property of an optical fiber; it affects the link budget and maximum unrepeated distance. The number and separation between optical repeaters and regenerators is largely determined by this loss. The mechanisms responsible for this loss include material absorption as well as both linear and nonlinear scattering of light from impurities in the fiber (1–5). Figure 13 illustrates some of the contributions to transmission loss in silica-based fibers as a function of wavelength in the near-infrared region, where optical loss is minimal and most optical communication systems operate. Typical loss for single-mode optical fiber is approximately 2 dB/km to 3 dB/km near a 800 nm wavelength, 0.5 dB/km near a 1300 nm wavelength, and 0.2 dB/km near a 1550 nm wavelength. Multimode fiber loss is slightly higher, and bending loss will only increase the link attenuation further.

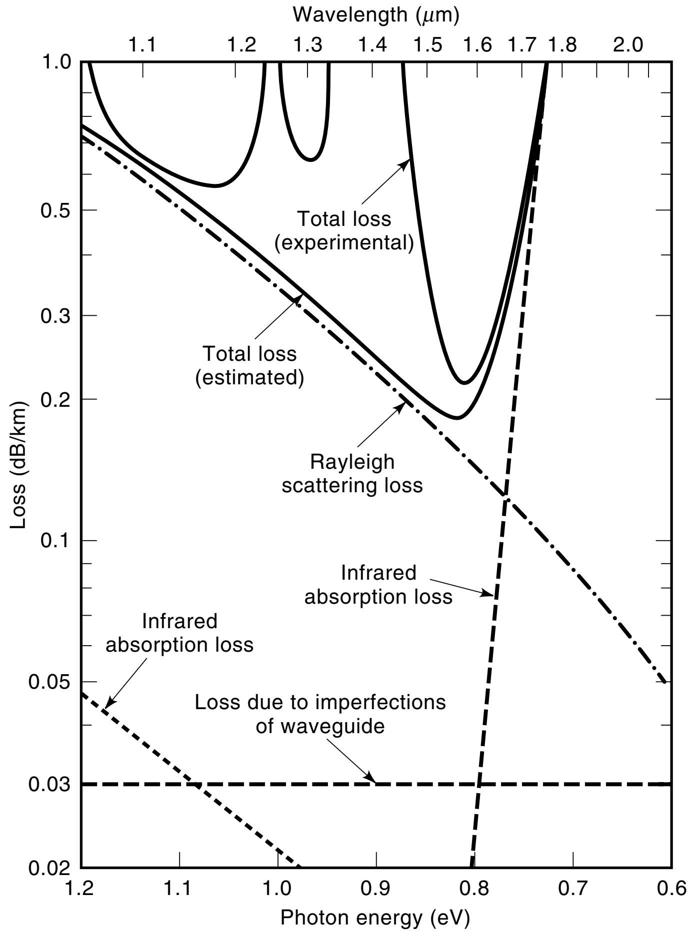

Figure 13. Transmission loss in silica-based optical fibers. Reprinted from Ref. 3, courtesy of Academic Press.

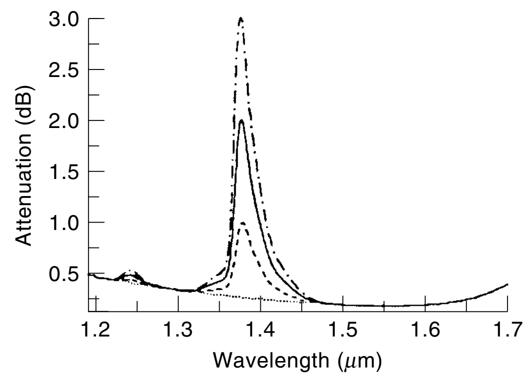

Figure 14. Attenuation versus wavelength of a singlemode fiber for different impurity levels. Attenuation peak near 1.4 μm increases with impurity concentration in fiber. Reprinted from Ref. 3, courtesy of Academic Press.

Attenuation versus Wavelength. Since fiber loss varies with wavelength, changes in the source wavelength or use of sources with a spectrum of wavelengths will produce additional loss. Transmission loss is minimized near the 1550 nm wavelength band, which unfortunately does not correspond with the dispersion minimum at around 1310 nm. An accurate model for fiber loss as a function of wavelength has been developed by Walker (18); this model accounts for the effects of linear scattering, macrobending, and material absorption from ultraviolet and infrared band edges, hydroxide (OH) absorption, and absorption from common impurities such as phosphorus. Using this model, it is possible to calculate the fiber loss as a function of wavelength for different impurity levels; an example of such a plot is shown in Fig. 14. Using this method, the fiber properties can be specified along with the acceptable wavelength limits of the source to limit the fiber loss over the entire operating wavelength range; design tradeoffs are possible between center wavelength and fiber composition to achieve the desired result. Typical loss due to wavelength-dependent attenuation for laser sources on single-mode fiber can be held below 0.1 dB/km.

Connector and Splice Loss. There are also installation losses associated with fiber optic connectors and splices; both of these are inherently statistical in nature and can be characterized by a Gaussian distribution. There are many different kinds of standardized optical connectors, some of which are shown in Fig. 15. Many different models which have been published for estimating connection loss from fiber misalignment (19,20); most of these treat loss from misalignment of fiber cores, offset of fibers on either side of the connector, and angular misalignment of fibers. The loss due to these effects is then combined into an overall estimate of the connector performance. There is no general model available to treat all types of connectors, but typical connector loss values average about 0.5 dB worst case for multimode, slightly higher for singlemode (see Table 3).

Optical splices are required for longer links, because fiber is usually available in spools of 1 to 5 km, or to repair broken fibers. There are two basic types, mechanical splices (which involve placing the two fiber ends in a receptacle that holds them close together, usually with epoxy) and the more commonly used fusion splices (in which the fibers are aligned, then heated sufficiently to fuse the two ends together). Typical splice loss values are given in Table 3.

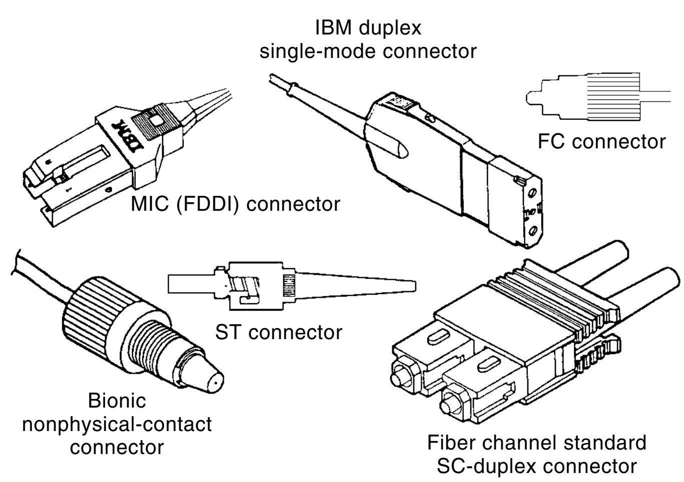

Figure 15. Common fiber optic connectors. Reprinted from Ref. 3, courtesy of Academic Press.

Table 3. Typical Fiberoptic Cable Plant Optical Losses

Component	Description	Size (μm)	Mean loss	Variance (dB^2)
Connector[a]	Physical contact	62.5–62.5	0.40 dB	0.02
		50.0–50.0	0.40 dB	0.02
		9.0–9.0[b]	0.35 dB	0.06
		62.5–50.0	2.10 dB	0.12
		50.0–62.5	0.00 dB	0.01
Connector[a]	Nonphysical contact (multimode only)	62.5–62.5	0.70 dB	0.04
		50.0–50.0	0.70 dB	0.04
		62.5–50.0	2.40 dB	0.12
		50.0–62.5	0.30 dB	0.01
Splice	Mechanical	62.5–62.5	0.15 dB	0.01
		50.0–50.0	0.15 dB	0.01
		9.0–9.0[b]	0.15 dB	0.01
Splice	Fusion	62.5–62.5	0.40 dB	0.01
		50.0–50.0	0.40 dB	0.01
		9.0–9.0[b]	0.40 dB	0.01
Cable	Multimode jumper	62.5	1.75 dB/km	NA
	Multimode jumper	50.0	3.00 dB/km at 850 nm	NA
	Single-mode jumper	9.0	0.8 dB/km	NA
	Trunk	62.5	1.00 dB/km	NA
	Trunk	50.0	0.90 dB/km	NA
	Trunk	9.0	0.50 dB/km	NA

[a] The connector loss value is typical when attaching identical connectors. The loss can vary significantly at attaching different connector types.
[b] Single-mode connectors and splices must meet a minimum return loss specification of 28 dB.
Reprinted from Ref. 3, courtesy of Academic Press.

Optical Power Penalties

Next, we consider the assembly loss budget, which is the difference between the transmitter output and receiver input powers, allowing for optical power penalties from noise sources in the link. Contributing factors include the following:

- Dispersion (modal and chromatic)
- Mode partition noise
- Mode hopping
- Extinction ratio
- Multipath interference
- Relative intensity noise (RIN)
- Timing jitter
- Radiation-induced darkening
- Modal noise
- Nonlinear effects (stimulated Raman and Brillouin scattering, frequency chirping)

Dispersion. The most important of these effects, and the most important fiber characteristic after transmission loss, is dispersion, or intersymbol interference. This refers to the broadening of optical pulses as they propagate along the fiber. As pulses broaden, they tend to interfere with adjacent pulses; this limits the data rate. In multimode fibers, there are two dominant kinds of dispersion: modal and chromatic. Modal dispersion refers to the fact that different modes travel at different velocities and cause pulse broadening. The fiber's modal bandwidth in units of megahertz per kilometer, is specified according to the expression

$$\mathrm{BW}_{\mathrm{modal}} = \mathrm{BW}_1/L^{\gamma} \tag{37}$$

where $\mathrm{BW}_{\mathrm{modal}}$ is the modal bandwidth for a length L of fiber, BW_1 is the manufacturer-specified modal bandwidth of a 1 km section of fiber, and γ is a constant known as the modal bandwidth concatenation length-scaling factor. The term γ usually assumes a value between 0.5 and 1, depending on details of the fiber manufacturing and design as well as the operating wavelength; it is conservative to take $\gamma = 1.0$. Modal bandwidth can be increased by mode mixing, which promotes the interchange of energy between modes to average out the effects of modal dispersion. Fiber splices tend to increase the modal bandwidth, although it is conservative to discard this effect when designing a link. There have been many attempts to fabricate fibers with enhanced modal bandwidth, most of which have not yet produced commercially viable products (1,21).

The other major contribution is chromatic dispersion, $\mathrm{BW}_{\mathrm{chrom}}$, which occurs because different wavelengths of light propagate at different velocities in the fiber. Put another way, the refractive index of the fiber is wavelength dependent; the fiber index depends on the fiber composition and may be calculated from the Sellmeier equation (1,3). For multimode fiber, chromatic bandwidth is given by an empirical model of the form

$$\mathrm{BW}_{\mathrm{chrom}} = \frac{L^{\gamma_c}}{\sqrt{\lambda_{\mathrm{w}}}(a_0 + a_1|\lambda_c - \lambda_{\mathrm{eff}}|)} \tag{38}$$

where L is the fiber length in km; λ_c is the center wavelength of the source in nm; λ_w is the source FWHM spectral width in nanometers; γ_c is the chromatic bandwidth length scaling coefficient, a constant; λ_{eff} is the effective wavelength, which combines the effects of the fiber zero dispersion wavelength and spectral loss signature; and the constants a_1 and a_0 are determined by a regression fit of measured data. From Ref. 22, the chromatic bandwidth for 62.5/125 μm fiber is empirically given by

$$\mathrm{BW}_{\mathrm{chrom}} = \frac{10^4 L^{-0.69}}{\sqrt{\lambda_{\mathrm{w}}}(1.1 + 0.0189|\lambda_{\mathrm{c}} - 1370|)} \tag{39}$$

For this expression, the center wavelength was 1335 nm and λ_{eff} was chosen midway between λ_{c} and the water absorption peak at 1390 nm; although λ_{eff} was estimated in this case, the expression still provides a good fit to the data. For 50/125 μm fiber, the expression becomes

$$\mathrm{BW}_{\mathrm{chrom}} = \frac{10^4 L^{-0.65}}{\sqrt{\lambda_{\mathrm{w}}}(1.01 + 0.0177|\lambda_{\mathrm{c}} - 1330|)} \tag{40}$$

For this case, λ_{c} was 1313 nm and the chromatic bandwidth peaked at $\lambda_{\mathrm{eff}} = 1330$ nm. Recall that this is only one possible model for fiber bandwidth (23). The total bandwidth capacity of multimode fiber BW_{t} is obtained by combining the modal and chromatic dispersion contributions, according to

$$\frac{1}{\mathrm{BW}_{\mathrm{t}}^2} = \frac{1}{\mathrm{BW}_{\mathrm{chrom}}^2} + \frac{1}{\mathrm{BW}_{\mathrm{modal}}^2} \tag{41}$$

Once the total bandwidth is known, the dispersion penalty can be calculated for a given data rate. One expression for the dispersion penalty in decibels is

$$P_{\mathrm{d}} = 1.22\left[\frac{\text{Bit Rate(Mb/s)}}{\mathrm{BW}_{\mathrm{t}}(\mathrm{MHz})}\right]^2 \tag{42}$$

For typical telecommunication grade fiber, the dispersion penalty for a 20 km link is about 0.5 dB. The graph of Fig. 16 shows the dispersion penalty as a function of the fiber bandwidth and length.

Dispersion is usually minimized at wavelengths near 1310 nm; special types of fiber have been developed that manipulate the index profile across the core to achieve minimal dispersion near 1550 nm, which is also the wavelength region of minimal transmission loss. Unfortunately, this dispersion-shifted fiber suffers from some practical drawbacks, including susceptibility to certain kinds of nonlinear noise and increased interference between adjacent channels in a wavelength-multiplexing environment. There is a new type of fiber that minimizes dispersion while reducing the unwanted cross-talk effects, called dispersion optimized fiber. By using a very sophisticated fiber profile, it is possible to minimize dispersion over the entire wavelength range from 1300 to 1550 nm, at the expense of very high loss (around 2 dB/km); this is known as dispersion-flattened fiber. Yet another approach is called dispersion-compensating fiber; this fiber is designed with negative dispersion characteristics, so that when used in series with conventional fiber it will undisperse the signal. Dispersion-compensating fiber has a much narrower core than standard single-mode fiber, which makes it susceptible to nonlinear effects; it is also birefringent and suffers from polarization mode dispersion, in which different states of polarized light propagate with very different group velocities. Note that standard single-mode fiber does not preserve the polarization state of the incident light; there is yet another type of specialty fiber, with asymmetric core profiles, capable of preserving the polarization of incident light over long distances.

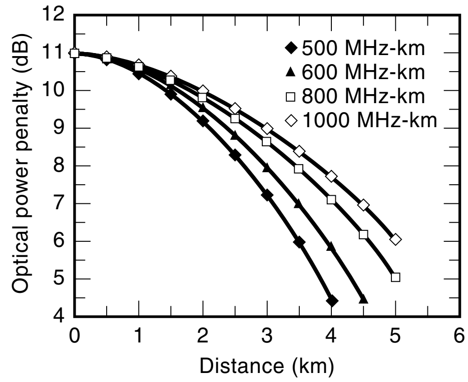

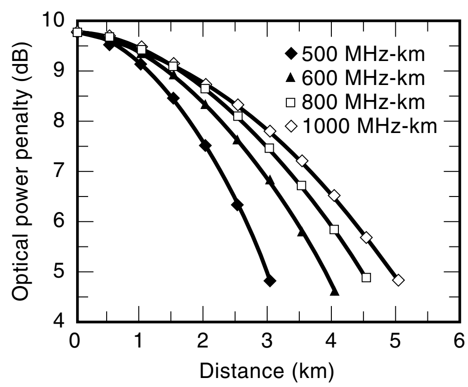

Figure 16. Dispersion penalty versus distance for different fiber bandwidths: (a) 50 μm fiber, (b) 62.5 μm fiber. Reprinted from Ref. 3, courtesy of Academic Press.

By definition, single-mode fiber does not suffer modal dispersion. Chromatic dispersion is an important effect, though, even given the relatively narrow spectral width of most laser diodes. The dispersion of single-mode fiber corresponds to the first derivative of group velocity τ_{g} with respect to wavelength and is given by

$$D = \frac{d\tau_{\mathrm{g}}}{d\lambda} = \frac{S_0}{4}\left(\lambda_{\mathrm{c}} - \frac{\lambda_0^4}{\lambda_{\mathrm{c}}^3}\right) \tag{43}$$

where D is the dispersion [in ps/km $\cdot$ nm^{-1}] and λ_{c} is the laser center wavelength. The fiber is characterized by its zero dispersion wavelength, λ_0, and zero dispersion slope, S_0. Usually, both center wavelength and zero dispersion wavelength are specified over a range of values; it is necessary to consider both upper and lower bounds in order to determine the worst-case dispersion penalty. This can be seen from Fig. 17, which plots D against wavelength for some typical values of λ_0 and λ_{c}; the largest absolute value of D occurs at the extremes of this region.

Once the dispersion is determined, the intersymbol interference penalty as a function of link length, L, can be deter-

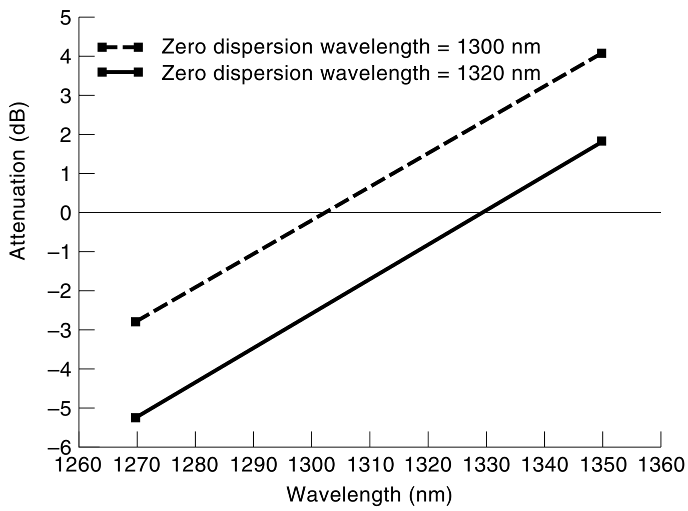

Figure 17. Single-mode fiber dispersion as a function of wavelength. Reprinted from Ref. 3, courtesy of Academic Press.

mined to a good approximation from a model proposed by Agrawal (24):

$$P_{\rm d} = 5\log(1 + 2\pi(BD\,\Delta\lambda)^2 L^2) \tag{44}$$

where B is the bit rate and $\Delta\lambda$ is the root mean square (rms) spectral width of the source. By maintaining a close match between the operating and zero dispersion wavelengths, this penalty can be kept to a tolerable 0.5 dB to 1.0 dB in most cases.

Mode Partition Noise. Group velocity dispersion contributes to another optical penalty that remains the subject of continuing research: mode partition noise and mode hopping. This penalty is related to the properties of a Fabry–Perot type laser diode cavity; although the total optical power output from the laser may remain constant, the optical power distribution among the laser's longitudinal modes will fluctuate. This is illustrated by the model depicted in Fig. 18; when a laser diode is directly modulated with injection current, the total output power stays constant from pulse to pulse; however, the power distribution among several longitudinal modes will vary between pulses. We must be careful to distinguish this behavior of the instantaneous laser spectrum, which varies with time, from the time-averaged spectrum, which is normally observed experimentally. The light propagates through a fiber with wavelength-dependent dispersion or attenuation, which deforms the pulse shape. Each mode is delayed by a different amount because of group velocity dispersion in the fiber; this leads to additional signal degradation at the receiver, in addition to the intersymbol interference caused by chromatic dispersion alone, which was discussed earlier. This is known as mode partition noise; it is capable of generating BER floors, such that additional optical power into the receiver will not improve the link BER. This is because mode partition noise is a function of the laser spectral fluctuations and wavelength-dependent dispersion of the fiber, so the signal-to-noise ratio due to this effect is independent of the signal power.

The power penalty caused by mode partition noise was first calculated by Ogawa (25) as

$$P_{\rm mp} = 5\log(1 - Q^2\sigma_{\rm mp}^2) \tag{45}$$

where

$$\sigma_{\rm mp}^2 = \frac{1}{2}k^2(\pi B)^4[A_1^4\Delta\lambda^4 + 42A_1^2A_2^2\Delta\lambda^6 + 48A_2^4\Delta\lambda^8] \tag{46}$$

$$A_1 = DL \tag{47}$$

and

$$A_2 = \frac{A_1}{2(\lambda_{\rm c} - \lambda_0)} \tag{48}$$

The mode partition coefficient, k, is a number between 0 and 1 that describes how much of the optical power is randomly shared between modes; it summarizes the statistical nature of mode partition noise. According to Ogawa, k depends on the number of interacting modes and rms spectral width of the source, the exact dependence being complex. However, subsequent work (26) has shown that Ogawa's model tends to underestimate the power penalty from mode partition noise, because it does not consider the variation of longitudinal mode power between successive baud periods

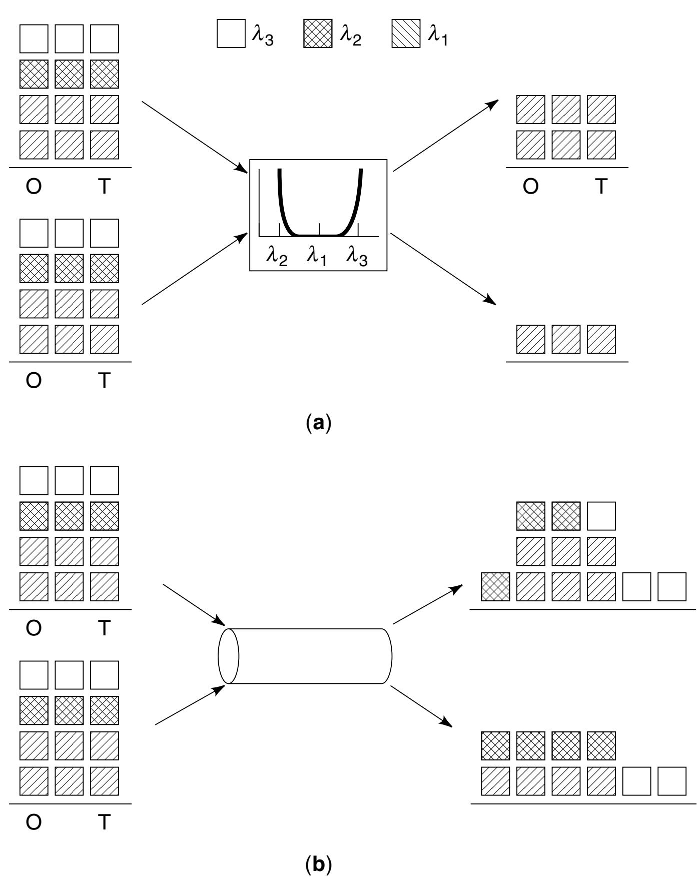

Figure 18. Model for mode partition noise; an optical source emits different wavelengths, illustrated by different shaded blocks: (a) wavelength-dependent loss, (b) chromatic dispersion. Reprinted from Ref. 3, courtesy of Academic Press.

and because it assumes a linear model of chromatic dispersion rather than the nonlinear model given in the above equation. A more detailed model has been proposed by Campbell (27), which is general enough to include effects of the laser diode spectrum, pulse shaping, transmitter extinction ratio, and statistics of the datastream. While Ogawa's model assumed an equiprobable distribution of zeros and ones in the datastream, Campbell showed that mode partition noise is data dependent as well. Recent work based on this model (28) has rederived the signal variance:

$$\sigma_{\mathrm{mp}}^2 = E_{\mathrm{av}}(\sigma_0^2 + \sigma_{+1}^2 + \sigma_{-1}^2) \tag{49}$$

where the mode partition noise contributed by adjacent baud periods is defined by

$$\sigma_{+1}^2 + \sigma_{-1}^2 = \frac{1}{2}k^2(\pi B)^4 [1.25A_1^4\Delta\lambda^4 + 40.95A_1^2A_2^2\Delta\lambda^6 + 50.25A_2^4\Delta\lambda^8] \tag{50}$$

and the time-average extinction ratio $E_{\mathrm{av}} = 10\log(P_1/P_0)$, where P_1, P_0 represent the optical power by a "1" and "0," respectively. If the operating wavelength is far from the zero dispersion wavelength, the noise variance simplifies to

$$\sigma_{mp}^2 = 2.25\frac{k^2}{2}E_{\mathrm{av}}(1-e^{-\beta L^2})^2 \tag{51}$$

which is valid provided that

$$\beta = (\pi BD\Delta\lambda)^2 \ll 1 \tag{52}$$

Many diode lasers exhibit mode hopping or mode splitting in which the spectrum appears to split optical power between two or three modes for brief periods of time. The exact mechanism is not fully understood, but stable Gaussian spectra are generally only observed for continuous operation and temperature-stabilized lasers. During these mode hops the above theory does not apply, because the spectrum is non-Gaussian, and the model will overpredict the power penalty; hence, it is not possible to model mode hops as mode partitioning with $k = 1$. There is no currently published model describing a treatment of mode hopping noise, although recent papers (29) suggest approximate calculations based on the statistical properties of the laser cavity. In a practical link, some amount of mode hopping is probably unavoidable as a contributor to burst noise; empirical testing of link hardware remains the only reliable way to reduce this effect.

Extinction Ratio. The receiver extinction ratio also contributes directly to the link penalties. The receiver BER is a function of the modulated ac signal power; if the laser transmitter has a small extinction ratio, the dc component of total optical power is significant. Gain or loss can be introduced in the link budget if the extinction ratio at which the receiver sensitivity is measured differs from the worst-case transmitter extinction ratio. If the extinction ratio E_t at the transmitter is defined as the ratio of optical power when a one is transmitted versus when a zero is transmitted,

$$E_t = \frac{\mathrm{Power}(1)}{\mathrm{Power}(0)}, \tag{53}$$

then we can define a modulation index at the transmitter M_t according to

$$M_t = \frac{E_t - 1}{E_t + 1} \tag{54}$$

Similarly, we can measure the linear extinction ratio at the optical receiver input and define a modulation index M_r. The extinction ratio penalty is given by

$$P_{\mathrm{er}} = -10\log\left(\frac{M_t}{M_r}\right) \tag{55}$$

where the subscripts t and r refer to specifications for the transmitter and receiver, respectively.

Multipath Interference. Another important property of the optical link is the amount of reflected light from the fiber endfaces that returns up the link back into the transmitter. Whenever there is a connection or splice in the link, some fraction of the light is reflected back; each connection is thus a potential noise generator, because the reflected fields can interfere with one another to create noise in the detected optical signal. The phenomenon is analogous to the noise caused by multiple atmospheric reflections of radio waves and is known as multipath interference noise. To limit this noise, connectors and splices are specified with a minimum return loss. If there are a total of N reflection points in a link and the geometric mean of the connector reflections is α, then based on the model of Ref. 30 the power penalty due to multipath interference (adjusted for BER and bandwidth) is closely approximated by

$$P_{\mathrm{mpi}} = 10\log(1 - 0.7N\alpha) \tag{56}$$

Multipath noise can usually be reduced well below 0.5 dB with available connectors, whose return loss is often better than 25 dB.

Relative Intensity Noise. Stray light reflected back into a Fabry–Perot type laser diode gives rise to intensity fluctuations in the laser output. This is a complicated phenomenon, strongly dependent on the type of laser; it is called either reflection-induced intensity noise or relative intensity noise (RIN). This effect is important, because it can also generate BER floors. The power penalty due to RIN is the subject of ongoing research; since the reflected light is measured at a specified signal level, RIN is data dependent, although it is independent of link length. Since many laser diodes are packaged in windowed containers, it is difficult to correlate the RIN measurements on an unpackaged laser with those of a commercial product. There have been several detailed attempts to characterize RIN (31,32); typically, the RIN noise is assumed Gaussian in amplitude and uniform in frequency over the receiver bandwidth of interest. The RIN value is specified for a given laser by measuring changes in the optical power when a controlled amount of light is fed back into the laser; it is signal dependent and is also influenced by temperature, bias voltage, laser structure, and other factors that typically influence laser output power (32).

If we assume that the effect of RIN is to produce an equivalent noise current at the receiver, then the additional receiver noise σ_r may be modeled as

$$\sigma_r = \gamma^2 S^{2g} B \tag{57}$$

where S is the signal level during a bit period, B is the bit rate, and g is a noise exponent that defines the amount of signal-dependent noise. If $g = 0$ noise power is independent of the signal, whereas if $g = 1$ noise power is proportional to the square of the signal strength. The coefficient γ is given by

$$\gamma^2 = S^{2(1-g)} \mathrm{i}\, 10^{(\mathrm{RIN_i}/10)} \tag{58}$$

where $\mathrm{RIN_i}$ is the measured RIN value at the average signal level S_i, including worst-case backreflection conditions and operating temperatures. The Gaussian BER probability due to the additional RIN noise current is given by

$$P_{\mathrm{error}} = \frac{1}{2}\left[P_e^1\left(\frac{S_1 - S_0}{2\sigma_1}\right) + P_e^0\left(\frac{S_1 - S_0}{2\sigma_0}\right)\right] \tag{59}$$

where σ_1, σ_0 represent the total noise current during transmission of a digital "1" and "0," respectively and P_e^1, P_e^0 are the probabilities of error during transmission of a "1" or "0," respectively.

The power penalty due to RIN may then be calculated by determining the additional signal power required to achieve the same BER with RIN noise present as without RIN present. One approximation for the RIN power penalty is given by

$$P_{\mathrm{RIN}} = -5\log\left[1 - Q^2(\mathrm{BW})(1+M_r)^{2g}(10^{\mathrm{RIN10}})\left(\frac{1}{M_r}\right)^2\right] \tag{60}$$

where the RIN value is specified (in decibels per Hertz), BW is the receiver bandwidth, M_r is the receiver modulation index, and the exponent g is a constant varying between 0 and 1 that relates the magnitude of RIN noise to the optical power level.

Jitter. Another important area in link design deals with the effects of timing jitter on the optical signal. In a typical optical link, a clock is extracted from the incoming data signal, which is used to retime and reshape the received digital pulse; the received pulse is then compared with a threshold to determine if a digital 1 or 0 was transmitted. So far, we have discussed BER testing with the implicit assumption that the measurement was made in the center of the received data bit; to achieve this, a clock transition at the center of the bit is required. When the clock is generated from a receiver timing recovery circuit, it will have some variation in time and the exact location of the clock edge will be uncertain. Even if the clock is positioned at the center of the bit, its position may drift over time. There will be a region of the bit interval, or eye, in the time domain where the BER is acceptable; this region is defined as the eyewidth (1–3).

Eyewidth measurements are an important parameter for evaluation of fiber optic links; they are intimately related to the BER, as well as the acceptable clock drift, pulse width distortion, and optical power. At low optical power levels, the receiver signal-to-noise ratio is reduced; increased noise causes amplitude variations in the received signal. These amplitude variations are translated into time domain variations in the receiver decision circuitry, which narrows the eyewidth. At the other extreme, an optical receiver may become saturated at high optical power, reducing the eyewidth and making the system more sensitive to timing jitter. This behavior results in the typical bathtub-shaped curve shown in Fig. 12; for this measurement, the clock is delayed from one end of the bit cell to the other, with the BER calculated at each position. Near the ends of the cell, a large number of errors occur; toward the center of the cell, the BER decreases to its true value. The eye opening may be defined as the portion of the eye for which the BER remains constant; pulse width distortion occurs near the edges of the eye, which denotes the limits of the valid clock timing. Uncertainty in the data pulse arrival times causes errors to occur by closing the eye window and causing the eye pattern to be sampled away from the center. This is one of the fundamental problems of optical and digital signal processing, and a large body of work has been published in this area (e.g., 33,34). In general, multiple jitter sources will be present in a link, which tend to be uncorrelated. However, jitter on digital signals, especially resulting from a cascade of repeaters, may be coherent.

The Commission for International Communications by Telephone and Telegraph (CCITT) (now known as the International Telecommunications Union, or ITU) has adopted a standard definition of jitter (34) as short-term variations of the significant instants (rising or falling edges) of a digital signal from their ideal position in time. Longer-term variations are described as wander; in terms of frequency, the distinction between jitter and wander is somewhat unclear. The predominant sources of jitter include the following:

1. Phase noise in receiver clock recovery circuits, particularly crystal-controlled oscillator circuits may be aggravated by filters or other components that do not have a linear phase response. Noise in digital logic resulting from restricted rise and fall times may also contribute to jitter.
2. Imperfect timing recovery in digital regenerative repeaters is usually dependent on the data pattern.
3. Different data patterns may contribute to jitter when the clock recovery circuit of a repeater attempts to recover the receive clock from inbound data. Data pattern sensitivity can produce as much as a 0.5 dB penalty in receiver sensitivity. Higher data rates are more susceptible (>1 Gbit/s); data patterns with long run lengths of 1s or 0s, or with abrupt phase transitions between consecutive blocks of 1s and 0s, tend to produce worst-case jitter.
4. At low optical power levels, the receiver signal-to-noise ratio, Q, is reduced; increased noise causes amplitude variations in the signal, which may be translated into time domain variations by the receiver circuitry.
5. Low frequency jitter, also called wander results from instabilities in clock sources and modulation of transmitters.
6. Very low frequency jitter can be caused by variations in the propagation delay of fibers, connectors, and so on, typically resulting from small temperature variations.

This can make it especially difficult to perform long-term jitter measurements.

In general, jitter from each of these sources will be uncorrelated; jitter related to modulation components of the digital signal may be coherent, and cumulative jitter from a series of repeaters or regenerators may also contain some well-correlated components.

There are several parameters of interest in characterizing jitter performance. Jitter may be classified as either random or deterministic, depending on whether it is associated with pattern-dependent effects; these are distinct from the duty cycle distortion which often accompanies imperfect signal timing. Each component of the optical link (data source, serializer, transmitter, encoder, fiber, receiver, retiming/clock recovery/deserialization, decision circuit) will contribute some fraction of the total system jitter. If we consider the link to be a black box (but not necessarily a linear system) then we can measure the level of output jitter in the absence of input jitter; this is known as the *intrinsic jitter* of the link. The relative importance of jitter from different sources may be evaluated by measuring the spectral density of the jitter. Another approach is the maximum tolerable input jitter (MTIJ) for the link. Finally, since jitter is essentially a stochastic process, we may attempt to characterize the jitter transfer function (JTF) of the link, or estimate the probability density function of the jitter. When multiple traces occur at the edges of the eye, this can indicate the presence of data-dependent jitter or duty-cycle distortion; a histogram of the edge location will show several distinct peaks. This type of jitter can indicate a design flaw in the transmitter or receiver. By contrast, random jitter typically has a more Gaussian profile and is present to some degree in all data links. All of these approaches have their advantages and drawbacks.

One of the first attempts to model the optical power penalty due to jitter (35) considered the general case of a receiver whose input was a raised cosine signal of the form

$$S_{\mathrm{t}} = \frac{1}{2}\,[1+\cos(\pi Bt)] \tag{61}$$

where B is the bit rate. A decision circuit samples this signal at some interval $t = n/B$. In the presence of random timing jitter, the sampling point fluctuates and the jitter-induced noise depends on the probability density function (PDF) of the random timing fluctuations. Determination of the actual PDF is quite difficult; if we can approximate $Bt \ll 1$, then it has been derived (36) that for a uniform PDF, the jitter induced noise σ_{j} is given by

$$\sigma_{\mathrm{j}}^2 = \frac{4}{5}(\pi Bt/4)^4 \tag{62}$$

Whereas for the less conservative case of a Gaussian PDF in the same limit,

$$\sigma_{\mathrm{j}}^2 = 2(\pi Bt/4)^4 \tag{63}$$

The optical power penalty in decibels due to jitter noise is then given by

$$P_{\mathrm{j}} = -5\log(1-4Q^2\sigma_{\mathrm{i}}^2) \tag{64}$$

where Q is the Gaussian error function. Based on this expression, the penalty for a Gaussian system is much larger than for a uniform PDF; when $Bt = 0.35$, a BER floor appears at 1e-9.

However, it was subsequently shown that the approximation on Bt is very restrictive, and the actual PDF is far from Gaussian; indeed, it is given by

$$P_{\mathrm{error}} = \int_{-1/B}^{1/B} (\mathrm{PDF_j})Q\left(\frac{A\cos(\pi Bt)}{2\sigma_{\mathrm{j}}}\right)dt \tag{65}$$

where the probability density function of the jitter is included under the integral. Numerical integration of this PDF shows that the approximate results given above tend to underestimate the effects of Gaussian jitter and overestimate the effects of uniform jitter by over 2 dB. Using similar approximations, jitter power penalties have been derived for both PIN and avalanche photodiodes (37). An alternative modeling approach has been to derive a worst-case distribution for the PDF, which will provide an upper bound on the performance of the optical link and can be more easily evaluated for analytical purposes.

The problem of jitter accumulation in a chain of repeaters becomes increasingly complex; however, we can state some general rules of thumb. It has been shown that jitter can be generally divided into two components, one due to repetitive patterns and one due to random data (38). In receivers with phase-lock loop timing recovery circuits, repetitive data patterns tend to cause jitter accumulation, especially for long run lengths. This effect is commonly modeled as a second-order receiver transfer function; the jitter accumulates according to the relationship

$$\mathrm{Jitter} \propto N + \left(\frac{N}{\xi}L\right)^2 \tag{66}$$

where N is the number of identical repeaters and ξ is the loop-damping factor, specific to a given receiver circuit. For large ξ, jitter accumulates almost linearly with the number of repeaters, whereas for small ξ the accumulation is much more rapid. Jitter will also accumulate when the link is transferring random data; jitter due to random data is of two types, systematic and random. The classic model for systematic jitter accumulation in cascaded repeaters was published by Byrne (39). The Byrne model assumes cascaded identical timing recovery circuits; the general expression for the jitter power spectrum is given by

$$J_{\mathrm{s}}^N = J_{\mathrm{s}}\left|\prod_{k=1}^{N} H + k(f) + \prod_{k=2}^{N} H_k(f) + \cdots + H_k(f)\right|^2 \tag{67}$$

where J_{s} is the systematic jitter generated by each repeater and $H(f)$ is the jitter transfer function of each timing recovery circuit. The corresponding model for random jitter accumulation is

$$J_{\mathrm{s}}^N = J_{\mathrm{r}}\left[\prod_{k=1}^{N} |H_k(f)|^2 + \prod_{k=2}^{N} |H_k(f)|^2 + \cdots + |H_k(f)|^2\right] \tag{68}$$

where J_r is the random jitter generated by each repeater. The systematic and random jitter can be combined as rms quantities,

$$J_t^2 = (J_s^N)^2 + (J_r^N)^2 \quad (69)$$

so that J_t, the total jitter due to random jitter, may be obtained. This model has been generalized to networks consisting of different components (40), and to non-identical repeaters (41). Despite these considerations, for well-designed practical networks the basic results of the Byrne model remain valid for N nominally identical repeaters transmitting random data; that is, systematic jitter accumulates in proportion to $N^{1/2}$ and random jitter accumulates in proportion to $N^{1/4}$.

Modal Noise. An additional effect of lossy connectors and splices is modal noise. Because high-capacity optical links tend to use highly coherent laser transmitters, random coupling between fiber modes causes fluctuations in the optical power coupled through splices and connectors; this phenomena is known as modal noise (42). As one might expect, modal noise is worst when using laser sources in conjunction with multimode fiber; recent industry standards have allowed the use of short-wave lasers (750 nm to 850 nm) on 50 μm fiber which may experience this problem. Modal noise is usually considered to be nonexistent in single-mode systems. However, modal noise in single-mode fibers can arise when higher order modes are generated at imperfect connections or splices. If the lossy mode is not completely attenuated before it reaches the next connection, interference with the dominant mode may occur. The effects of modal noise have been modeled previously (42), assuming that the only significant interaction occurs between the LP_{01} and LP_{11} modes for a sufficiently coherent laser. For N sections of fiber, each of length L in a single-mode link, the worst case sigma for modal noise can be given by

$$\sigma_m = \sqrt{2}N\eta(1-\eta)e^{-aL} \quad (70)$$

where a is the attenuation coefficient of the LP_{11} mode, and η is the splice transmission efficiency, given by

$$\eta = 10^{-(\eta_0/10)} \quad (71)$$

where η_0 is the mean splice loss (typically, splice transmission efficiency will exceed 90%). The corresponding optical power penalty due to modal noise is given by

$$P = -5\log(1 - Q^2\,\sigma_m^2) \quad (72)$$

where Q corresponds to the desired BER.

Radiation-Induced Loss. Another important environmental factor as mentioned earlier is exposure of the fiber to ionizing radiation damage. There is a large body of literature concerning the effects of ionizing radiation on fiber links (43,44). Many factors can affect the radiation susceptibility of optical fiber, including the type of fiber, type of radiation (gamma radiation is usually assumed to be representative), total dose, dose rate (important only for higher exposure levels), prior irradiation history of the fiber, temperature, wavelength, and data rate. Optical fiber with a pure silica core is least susceptible to radiation damage; however, almost all commercial fiber is intentionally doped to control the refractive index and dispersion properties of the core and cladding. Trace impurities are also introduced, which become important only under irradiation; among the most important are germanium dopants in the core of graded index (GRIN) fibers, in addition to flourine, chlorine, phosphorus, boron, and hydroxide content, and the alkali metals. In general, radiation sensitivity is worst at lower temperatures, and is also made worse by hydrogen diffusion from materials in the fiber cladding. Because of the many factors involved, there does not exist a comprehensive theory to model radiation damage in optical fibers. The basic physics of the interaction has been described elsewhere (43,44); there are two dominant mechanisms, radiation-induced darkening and scintillation. First, high-energy radiation can interact with dopants, impurities, or defects in the glass structure to produce color centers that absorb strongly at the operating wavelength. Carriers can also be freed by radiolytic or photochemical processes; some of these become trapped at defect sites, which modifies the band structure of the fiber and causes strong absorption at infrared wavelengths. This radiation-induced darkening increases the fiber attenuation; in some cases, it is partially reversible when the radiation is removed, although high levels or prolonged exposure will permanently damage the fiber. A second effect is caused if the radiation interacts with impurities to produce stray light or scintillation. This light is generally broadband but will tend to degrade the BER at the receiver; scintillation is a weaker effect than radiation-induced darkening. These effects will degrade the BER of a link. However, they can be prevented by shielding the fiber or partially overcome by a third mechanism, photobleaching. The presence of intense light at the proper wavelength can partially reverse the effects of darkening in a fiber. It is also possible to treat silica core fibers by briefly exposing them to controlled levels of radiation at controlled temperatures, which increases the fiber loss, but makes the fiber less susceptible to future irradiation. These so-called radiation-hardened fibers are often used in environments where radiation is anticipated to play an important role. Recently, several models have been advanced for the performance of fiber under moderate radiation levels (44); the effect on BER is a power law model of the form

$$\mathrm{BER} = \mathrm{BER}_0 + A(\mathrm{dose})^b \quad (73)$$

where BER_0 is the link BER prior to irradiation, the dose is given in rads, and the constants A and b are empirically fitted. The loss due to normal background radiation exposure over a typical link lifetime can be held below about 0.5 dB.

Stimulated Brillouin and Raman Scattering. At high optical power levels, nonlinear effects in the fiber may limit the link performance. The dominant effects are stimulated Raman and Brillouin scattering. When incident optical power exceeds a threshold value, a significant amount of light scatters from small imperfections in the fiber core. The scattered light is frequency shifted, since the scattering process involves the generation of phonons (45). This is known as stimulated Brillouin scattering; under these conditions, the output light intensity becomes nonlinear, as well. When the scattered light experiences frequency shifts outside the acoustic phonon range, due instead to modulation by impurities or molecular vibrations in the fiber core, the effect is known as Raman scattering. Stimulated Brillouin scattering will not occur below the optical power threshold defined by

$$P_e = 21\,\frac{A}{G_b L_e}\,\mathrm{W} \tag{74}$$

where L_e is the effective interaction length, A is the cross-sectional area of the guided mode, and G_b is the Brillouin gain coefficient. Similarly, Raman scattering will not occur unless the optical power exceeds the value given by

$$P_r = 16\,\frac{A}{G_r L}\,\mathrm{W} \tag{75}$$

where G_r is the Raman gains coefficient. Brillouin scattering has been observed in single-mode fibers at wavelengths greater than cutoff with optical power as low as 5 mW; a good rule of thumb is that the Raman scattering threshold is approximately three times larger than the Brillouin threshold. As a general guide, the optical power threshold for Brillouin scattering in singlemode fiber is approximately 10 mW and for Raman scattering is approximately 3.5 W. These effects rarely occur in multimode fiber, where the thresholds for Brillouin and Raman scattering are approximately 450 mW and 150 W, respectively.

Frequency Chirp. The final nonlinear effect that we consider is frequency chirping of the optical signal. Chirping refers to a change in frequency with time, and takes its name from the sound of an acoustic signal whose frequency increases or decreases linearly with time. There are three ways in which chirping can affect a fiber optic link. First, the laser transmitter can be chirped as a result of physical processes within the laser (46); the effect has its origin in carrier-induced refractive index changes, making it an inevitable consequence of high power direct modulation of semiconductor lasers. For lasers with low levels of relaxation oscillation damping, a model has been proposed for the chirped power penalty:

$$P = 10\log\left(1 + \frac{\pi B^2 \lambda^2 L D a}{4c}\right) \tag{76}$$

where c is the speed of light, B is the fiber bandwidth, λ is the wavelength of light, L is the length of the fiber, D is the dispersion, and a is the linewidth enhancement factor (a typical value is -4.5); this model is only a first approximation, because it neglects the dependence of chirp on extinction ratio and nonlinear effects such as spectral hole burning. Secondly, a sufficiently intense light pulse is chirped by the nonlinear process of self-phase modulation in an optical fiber (47). This carrier-induced phase modulation arises from the interaction of the light and the intensity dependent portion of the fiber's refractive index (known as the Kerr effect); it is thus dependent on the material and structure of the fiber, polarization of the light, and the shape of the incident optical pulse. If different wavelengths are present in the same fiber, the effect caused by one signal can induce cross-phase modulation in the others. Based on a model by Stolen and Lin (47), the maximum optical power level before the spectral width increases by 2 nm is given by

$$P = \frac{n^2 A}{377 n_2 \kappa L_e}\,\mathrm{W} \tag{77}$$

where

$$L_e = (1/a_0)[1 - \exp(-a_0 L)] \tag{78}$$

where n is the fiber's refractive index, κ is the propagation constant (a typical value is 7×10^4 at a wavelength of 1.3 μm), a_0 is the fiber attenuation coefficient, A is the fiber core cross-sectional area, n_2 is the nonlinear coefficient of the fiber's refractive index (a typical value is 6.1×10^{-19}), and L_e is the effective interaction length for the nonlinear interaction, which is related to the actual length of the fiber, L, by Eq. (78). This expression should be multiplied by 5/6 if the fiber is not polarization preserving. Typically, this effect is not significant for optical power levels less than 950 mW in a singlemode fiber at 1.3 μm wavelength. Finally, there is a power penalty arising from the propagation of a chirped optical pulse in a dispersive fiber, because the new frequency components propagate at different group velocities. This may be treated as simply a much worse case of the conventional dispersion penalty, provided that one of the first two effects exists to chirp the optical signal.

OPTICAL LINK STANDARDS

In the past 10 years there have been several international standards adopted for optical communications. This section presents a brief overview of several major industry standards, including the following: ESCON/SBCON (Enterprise System Connection / Serial Byte Connectivity), FDDI (Fiber Distributed Data Interface), Fibre Channel Standard, ATM (Asynchronous Transfer Mode)/SONET (Synchronous Optical Network), and Gigabit Ethernet.

ESCON

The Enterprise System Connection (ESCON) architecture was introduced on the IBM System/390 family of mainframe computers in 1990 (ESCON is a registered trademark of IBM Corporation) as an alternative high-speed input–output channel attachment (48,49). The ESCON interface specifications were adopted in 1996 by the ANSI X3T1 committee as the Serial Byte Connection (SBCON) standard (50).

The ESCON/SBCON channel is a bidirectional, point-to-point 1300 nm fiber optic data link with a maximum data rate of 17 Mbyte/s (200 Mbit/s). ESCON supports a maximum unrepeated distance of 3 km using 62.5 μm multimode fiber and LED transmitters with an 8 dB link budget, or a maximum unrepeated distance of 20 km using singlemode fiber and laser transmitters with a 14 dB link budget. The laser channels are also known as the ESCON Extended Distance Feature (XDF). Physical connection is provided by an ESCON duplex connector (Fig. 15). Recently, the singlemode ESCON links have adopted the SC duplex connector as standardized by Fibre Channel (Fig. 15). With the use of repeaters or switches, an ESCON link can be extended up to 3 to 5 times these distances; however, performance of the attached devices typically falls off quickly at longer distances due to the longer round-trip latency of the link, making this approach suitable only for applications that can tolerate a lower effective throughput, such as remote backup of data for disaster recovery. ESCON devices and CPUs may communicate directly through a channel-to-channel attachment, but more commonly attach to a central nonblocking dynamic cross-point switch. The resulting network topology is similar to a star-wired ring, which provides both efficient bandwidth utilization and reduced cabling requirements. The switching function is provided by an ESCON Director, a nonblocking circuit switch. Although ESCON uses 8B/10B encoded data, it is not a packet switching network; instead, the data frame header includes a request for connection that is established by the Director for the duration of the data transfer. An ESCON data frame includes a header, payload of up to 1028 bytes of data, and a trailer. The header consists of a two character start-of-frame delimiter, two byte destination address, two byte source address, and one byte of link control information. The trailer is a two byte cyclic redundancy check (CRC) for errors and a three character end-of-frame delimiter. ESCON uses a DC-balanced 8B/10B coding scheme developed by IBM.

FDDI

The fiber distributed data interface (FDDI) was among the first open networking standards to specify optical fiber. It was an outgrowth of the ANSI X3T9.5 committee proposal in 1982 for a high-speed token passing ring as a back-end interface for storage devices. Although interest in this application waned, FDDI found new applications as the backbone for local area networks (LANs). The FDDI standard was approved in 1992 as ISO standards IS 9314/1-2 and DIS 9314-3; it follows that the architectural concepts of IEEE standard 802 (although it is controlled by ANSI, not IEEE, and therefore has a different numbering sequence) and is among the family of standards including token ring and Ethernet which are compatible with a common IEEE 802.2 interface. FDDI is a family of four specifications, namely the physical layer (PHY), physical media dependent (PMD), media access control (MAC), and station management (SMT). These four specifications correspond to sublayers of the Data Link and Physical Layer of the OSI reference model; as before, we concentrate on the physical layer implementation.

The FDDI network is a 100 Mbit/s token passing ring, with dual counter-rotating rings for fault tolerance. The dual rings are independent fiber optic cables; the primary ring is used for data transmission, and the secondary ring is a backup in case a node or link on the primary ring fails. Bypass switches are also supported to reroute traffic around a damaged area of the network and prevent the ring from fragmenting in case of multiple node failures. The actual data rate is 125 Mbit/s, but this is reduced to an effective data rate of 100 Mbit/s by using a 4B/5B coding scheme. This high-speed allows FDDI to be used as a backbone to encapsulate lower speed 4, 10, and 16 Mbit/s LAN protocols; existing Ethernet, token ring, or other LANs can be linked to an FDDI network via a bridge or router. Although FDDI data flows in a logical ring, a more typical physical layout is a star configuration with all nodes connected to a central hub or concentrator rather than to the backbone itself. There are two types of FDDI nodes, either dual attach (connected to both rings) or single attach; a network supports up to 500 dual attached nodes, 1000 single attached nodes, or an equivalent mix of the two types. FDDI specifies 1300 nm LED transmitters operating over 62.5 μm multimode fiber as the reference media, although the standard also provides for the attachment of 50, 100, 140, and 85 μm fiber. Using 62.5 μm fiber, a maximum distance of 2 km between nodes is supported with an 11 dB link budget; because each node acts like a repeater with its own phase-lock loop to prevent jitter accumulation, the entire FDDI ring can be as large as 100 km. However, an FDDI link can fail due to either excessive attenuation or dispersion; for example, insertion of a bypass switch increases the link length and may cause dispersion errors even if the loss budget is within specifications. For most other applications, this does not occur because the dispersion penalty is included in the link budget calculations or the receiver sensitivity measurements. The physical interface is provided by a special Media Interface Connector (MIC), illustrated in Fig. 15. The connector has a set of three color-coded keys which are interchangeable depending on the type of network connection (1); this is intended to prevent installation errors and assist in cable management.

An FDDI data frame has variable length, and contains up to 4500 8-bit bytes, or octets, including a preamble, start of frame, frame control, destination address, data payload, CRC error check, and frame status/end of frame. Each node has a MAC sublayer that reviews all the data frames looking for its own destination address. When it finds a packet destined for its node, that frame is copied into local memory, a copy bit is turned on in the packet, and it is then sent on to the next node on the ring. When the packet returns to the station that originally sent it, the originator assumes that the packet was received if the copy bit is on; the originator will then delete the packet from the ring. As in the IEEE 802.5 token ring protocol, a special type of packet called a token circulates in one direction around the ring and a node can only transmit data when it holds the token. Each node observes a token retention time limit, and also keeps track of the elapsed time since it last received the token; nodes may be given the token in equal turns, or they can be given priority by receiving it more often or holding it longer after they receive it. This allows devices having different data requirements to be served appropriately.

Because of the flexibility built into the FDDI standard, many changes to the base standard have been proposed to allow interoperability with other standards, reduce costs, or extend FDDI into the MAN or WAN. These include a singlemode PMD layer for channel extensions up to 20 km to 50 km. An alternative PMD provides for FDDI transmission over copper wire, either shielded or unshielded twisted pairs; this is known as copper distributed data interface, or CDDI. A new PMD is also being developed to adapt FDDI data packets for transfer over a SONET link by stuffing approximately 30 Mbit/s into each frame to make up for the data rate mismatch (we will discuss SONET as an ATM physical layer in a later section). An enhancement called FDDI-II uses time division multiplexing to divide the bandwidth between voice and data; it would accommodate isochronous, circuit-switched traffic as well as existing packet traffic. Recently, an option known as low cost FDDI has been adopted. This specification uses the more common SC duplex connector instead of the expensive

MIC connectors, and a lower cost transceiver with a 9 pin footprint similar to the singlemode ESCON parts.

Fibre Channel Standard

Development of the ANSI Fibre Channel Standard (FC) began in 1988 under the X3T9.3 Working Group, as an outgrowth of the Intelligent Physical Protocol Enhanced Physical Project. The motivation for this work was to develop a scaleable standard for the attachment of both networking and input–output devices using the same drivers, ports, and adapters over a single channel at the highest speeds currently achievable. The standard applies to both copper and fiber optic media, and uses the English spelling “fibre” to denote both types of physical layers. In an effort to simplify equipment design, FC provides the means for a large number of existing upper level protocols (ULPs), such as IP, SCI, and HIPPI, to operate over a variety of physical media. Different ULPs are mapped to FC constructs, encapsulated in FC frames, and transported across a network; this process remains transparent to the attached devices. The standard consists of five hierarchical layers (51), namely a physical layer, an encode–decode layer which has adopted the dc-balanced 8B/10B code, a framing protocol layer, a common services layer (at this time, no functions have been formally defined for this layer) and a protocol mapping layer to encapsulate ULPs into FC. The second layer defines the FC data frame; frame size depends upon the implementation, and is variable up to 2148 bytes long. Each frame consists of a 4 byte start of frame delimiter, a 24 byte header, a 2112 byte payload containing from 0 to 64 bytes of optional headers and 0 to 2048 bytes of data, a 4 byte CRC and a 4 byte end of frame delimiter. In October 1994, the FC physical and signaling interface standard FC-PH was approved as ANSI standard X3.230-1994.

Logically, FC is a bidirectional point-to-point serial data link. Physically, there are many different media options (see Table 4) and three basic network topologies. The simplest, default topology is a point-to-point direct link between two devices, such as a CPU and a device controller. The second, Fibre Channel Arbitrated Loop (FC-AL), connects between 2 and 126 devices in a loop configuration. Hubs or switches are not required, and there is no dedicated loop controller; all nodes on the loop share the bandwidth and arbitrate for temporary control of the loop at any given time. Each node has equal opportunity to gain control of the loop and establish a communications path, but once the node relinquishes control, a fairness algorithm insures that the same node cannot win control of the loop again until all other nodes have had a turn. As networks become larger, they may grow into the third topology, an interconnected switchable network or fabric in which all network management functions are taken over by a switching point, rather than each node. An analogy for a switched fabric is the telephone network; users specify an address (phone number) for a device with which they want to communicate, and the network provides them with an interconnection path. In theory there is no limit to the number of nodes in a fabric; practically, there are only about 16 million unique addresses. Fibre Channel also defines three classes of connection service, which offer options such as guaranteed delivery of messages in the order they were sent and acknowledgment of received messages.

As shown in Table 4, FC provides for both singlemode and multimode fiber optic data links using long-wave (1300 nm)

Table 4. Fibre Channel Media Performance

Media Type	Data Rate (Mb/s)	Max. Distance	Signaling Rate (Mbaud)	Transmitter
Single-mode fiber	100	10 km	1062.5	LW laser
	50	10 km	1062.5	LW laser
	25	10 km	1062.5	LW laser
50 μm multimode fiber	100	500 m	1062.5	SW laser
	50	1 km	531.25	SW laser
	25	2 km	265.625	SW laser
	12.5	10 km	132.8125	LW LED
62.5 μm multimode fiber	100	300 m	1062.5	SW laser
	50	600 m	531.25	SW laser
	25	1 km	265.625	LW LED
	12.5	2 km	132.8125	LW LED
105 Ω type-1 shielded twisted-pair electrical	25	50 m	265.125	ECL
	12.5	100 m	132.8125	ECL
75 Ω mini coax	100	10 m	1062.5	ECL
	50	20 m	531.25	ECL
	25	30 m	265.625	ECL
	12.5	40 m	132.8125	ECL
75 Ω video coax	100	25 m	1062.5	ECL
	50	50 m	531.25	ECL
	25	75 m	265.625	ECL
	12.5	100 m	132.8125	ECL
150 Ω twinax or STP	100	30 m	1062.5	ECL
	50	60 m	531.25	ECL
	25	100 m	265.625	ECL

Reprinted from Ref. 3, courtesy of Academic Press.

lasers and LEDs as well as short-wave (780 to 850 nm) lasers. The physical connection is provided by an SC duplex connector defined in the standard (see Fig. 15), which is keyed to prevent misplugging of a multimode cable into a singlemode receptacle. This connector design has since been adopted by other standards, including ATM, low cost FDDI, and singlemode ESCON. The requirement for international class 1 laser safety is addressed using open fiber control (OFC) on some types of multimode links with short-wave lasers. This technique automatically senses when a full duplex link is interrupted, and turns off the laser transmitters on both ends to preserve laser safety. The lasers then transmit low duty cycle optical pulses until the link is reestablished; a handshake sequence then automatically reactivates the transmitters.

ATM/SONET

Developed by the ATM Forum, this protocol has promised to provide a common transport medium for voice, data, video, and other types of multimedia. ATM is a high level protocol, which can run over many different physical layers including copper; part of ATM's promise to merge voice and data traffic on a single network comes from plans to run ATM over the Synchronous Optical Network (SONET) transmission hierarchy developed for the telecommunications industry. SONET is really a family of standards defined by ANSI T1.105-1988 and T1.106-1988, as well as by several CCITT recommendations (52–55). Several different data rates are defined as multiples of 51.84 Mbit/s, known as OC-1. The numerical part of the OC-level designation indicates a multiple of this fundamental data rate, thus, 155 Mbit/s is called OC-3 (see Table 5). The standard provides for seven incremental data rates, OC-3, OC-9, OC-12, OC-18, OC-24, OC-36, and OC-48 (2.48832 Gbit/s). Both singlemode links with laser sources and multimode links with LED sources are defined for OC-1 through OC-12; only singlemode laser links are defined for OC-18 and beyond. In addition to the specifications in Table 5, SONET also contains provisions to carry sub-OC-1 data rates, called virtual tributaries, which support telecom data rates including DS-1 (1.544 Mbit/s), DS-2 (6.312 Mbit/s), and DS1C (3.152 Mbit/s). The basic SONET data frame is an array of nine rows with 90 bytes per row, known as a synchronous-transport-signal level 1 (STS-1) frame. In an OC-1 system, an STS-1 frame is transmitted once every 125 μs (810 bytes per 125 μs yields 51.84 Mbit/s). The first three columns provide overhead functions such as identification, framing, error checking, and a pointer to identify the start of the 87 byte data payload. The payload floats in the STS-1 frame, and may be split across two consecutive frames. Higher speeds can be obtained either by concatenation of N frames into an STS-N_c frame (the "c" stands for "concatenated") or by byte interleaved multiplexing of N frames into an STS-N frame.

ATM technology incorporates elements of both circuit and packet switching. All data are broken down into a 53 byte cell, which may be viewed as a short-fixed-length packet. Five bytes make up the header, providing a 48 byte payload. The header information contains routing information (cell addresses) in the form of virtual path and channel identifiers, a field to identify the payload type, an error check on the header information, and other flow control information. Cells are generated asynchronously; as the data source provides enough information to fill a cell, it is placed in the next available cell slot. There is no fixed relationship between the cells and a master clock, as in conventional time division multiplexing schemes; the flow of cells is driven by the bandwidth needs of the source. ATM provides bandwidth on demand; for example, in a client-server application the data may come in bursts; several data sources could share a common link by multiplexing during the idle intervals. Thus, the ATM adaptation layer allows for both constant and variable bit rate services. The combination of transmission options is sometimes described as a pleisosynchronous network, meaning that it combines some features of multiplexing operations without requiring a fully synchronous implementation. Note that the

Table 5. SONET Physical Layer Optical Specifications

Parameter	Units	OC-1	OC-3	OC-9	OC-12	OC-18	OC-24	OC-36	OC-48
Data rate									
Bit rate	Mb/s	51.84	155.52	455.56	622.08	933.12	1244.16	1866.24	2488.32
Tolerance	ppm			100					
Transmitter type		MLM/LED	MLM/LED	MLM/LED	MLM/LED	MLM	MLM	MLM	MLM
$\lambda_{W_{\min}}$	nm	1260	1260	1260	1260	1260	1260	1260	1265
$\lambda_{W_{\max}}$	nm	1360	1360	1360	1360	1360	1360	1360	1360
$\Delta\lambda_{\max}$	nm	80	40/80	19/45	14.5/35	9.5	7	4.8	5
$P_{T_{\max}}$	dBm	−14	−8	−8	−8	−8	−5	−3	−3
$P_{T_{\min}}$	dBm	−23	−15	−15	−15	−15	−12	−10	−10
$r_{c_{\min}}$	dB	8.2	8.2	8.2	8.2	8.2	8.2	8.2	8.2
Optical path system									
$ORL_{\max}$	dB	na	na	na	na	20	20	24	24
$D_{SR_{\max}}$	ps/nm	na	na	31/na	13/na	13	13	13	12
Max sndr. to rcvr. reflectance	dB	na	na	na	na	−25	−25	−27	−27
Receiver									
$P_{r_{\max}}$	dBm	−15	−8	−8	−8	−8	−5	−3	−3
$P_{r_{\min}}$	dBm	−31	−23	−23	−23	−23	−20	−18	−18
P_0	dBm	1	1	1	1	1	1	1	1

Reprinted from Ref. 3, courtesy of Academic Press.

fixed cell length allows the use of synchronous multiplexing and switching techniques, while the generation of cells on demand allows flexible use of the link bandwidth for different types of data, characteristic of packet switching. Higher level protocols may be required in an ATM network to insure that multiplexed cells arrive in the correct order or to check the data payload for errors (given the typical high reliability and low BER of modern fiber optic technology, it was considered unnecessary overhead to replicate data error checks at each node of an ATM network). If an intermediate node in an ATM network detects an error in the cell header, cells may be discarded without notification to either end user. Although cell loss priority may be defined in the ATM header, for some applications the adoption of unacknowledged transmission may be a concern.

ATM data rates were intended to match SONET rates of 51, 155, and 622 Mbit/s; an FDDI compliant data rate of 100 Mbit/s was added, to facilitate emulation of different types of LAN traffic over ATM. To provide a low-cost copper option and compatibility with 16 Mbit/s token ring LANs to the desktop, a 25 Mbit/s speed has also been approved. For premises wiring applications, ATM specifies the SC Duplex connector, color coded beige for multimode links and blue for singlemode links. At 155 Mbit/s, multimode ATM links support a maximum distance of 3 km while single-mode links support up to 20 km.

Gigabit Ethernet

Ethernet is a local area network (LAN) communication standard originally developed for copper interconnections on a common data bus; it is an IEEE standard 802.3 (56). The basic principle used in Ethernet is carrier sense multiple access with collision detection (CSMA/CD). Ethernet LANs are typically configured as a bus, often wired radially through a central hub. A device attached to the LAN that intends to transmit data must first sense whether another device is transmitting. If another device is already sending, then it must wait until the LAN is available; thus, the intention is that only one device will be using the LAN to send data at a given time. When one device is sending, all other attached devices receive the data and check to see if it is addressed to them; if it is not, then the data is discarded. If two devices attempt to send data at the same time (for example, both devices may begin transmission at the same time after determining that the LAN is available; there is a gap between when one device starts to send and before another potential sender can detect that the LAN is in use), then a collision occurs. Using CSMA/CD as the media access control protocol, when a collision is detected attached devices will detect the collision and must wait for different lengths of time before attempting retransmission. Since it is not always certain that data will reach its destination without errors or that the sending device will know about lost data, each station on the LAN must operate an end-to-end protocol for error recovery and data integrity. Data frames begin with an 8 byte preamble used for determining start-of-frame and synchronization, and a header consisting of a 6 byte destination address, 6 byte source address, and 2 byte length field. User data may vary from 46 to 1500 bytes, with data shorter than the minimum length padded to fit the frame; the user data is followed by a 2 byte CRC error check. Thus, an Ethernet frame may range from 70 bytes to 1524 bytes.

The original Ethernet standard, known also as 10Base-T (10 Mbit/s over unshielded twisted pair copper wires) was primarily a copper standard, although a specification using 850 nm LEDs was also available. Subsequent standardization efforts increased this data rate to 100 Mbit/s over the same copper media (100Base-T), while once again offering an alternative fiber specification (100Base-FX). Recently, the standard has continued to evolve with the development of gigabit Ethernet (1000Base-FX), which will operate over fiber as the primary medium; this has the potential to be the first networking standard for which the implementation cost on fiber is lower than on copper media. Currently under development as IEEE 802.3z, the gigabit Ethernet standard is scheduled for final approval in late 1998. Gigabit Ethernet will include some changes to the MAC layer in addition to a completely new physical layer operating at 1.25 Gbit/s. Switches rather than hubs are expected to predominate, since at higher data rates throughput per end user and total network cost are both optimized by using switched rather than shared media. The minimum frame size has increased to 512 bytes; frames shorter than this are padded with idle characters (carrier extension). The maximum frame size remains unchanged, although devices may now transmit multiple frames in bursts rather than single frames for improved efficiency. The physical layer will use standard 8B/10B data encoding. The physical layer specifications have not been finalized as of this writing. The standard does not specify a physical connector type for fiber; at this writing there are several proposals, including the SC duplex and various small-form factor connectors approximately the size of a standard RJ-45 jack, such as the MT-RJ, SC/DC, and SG connectors. Transceivers may be packaged as gigabit interface converters, or GBICs, which allows different optical or copper transceivers to be plugged onto the same host card. There is presently a concern with proposals to operate long-wave (1300 nm) laser sources over both singlemode and multimode fiber. When a transmitter is optimized for a singlemode launch condition, it will underfill the multimode fiber; this causes some modes to be excited and propagate at different speeds than others, and the resulting differential mode delay significantly degrades link performance. One proposed solution involves the use of special optical cables with offset ferrules to simulate an equilibrium mode launch condition into multimode fiber. The issue has not been resolved as of this writing.

ADVANCED TOPICS

In the following sections, several advanced topics under development in optical communications are presented, including the following: parallel optical interconnections, plastic optical fiber, wavelength division multiplexing (WDM), solitons, and optical amplifiers.

Parallel Optical Interconnect

In the quest for 2.5 Gbit/s data rates and beyond, one approach is to develop very-high-speed serial transceivers. Another approach, which may be more cost effective, involves striping several lower speed fibers in parallel; this space-division multiplexed approach is the motivation behind parallel optical interconnects (POI). Recent advances in vertical cavity surface emitting laser (VCSEL) arrays, optical fiber ribbon connectors, and receiver arrays have contributed to the commercialization of this technology. The first commercially available POI transceiver was the Motorola Optobus, announced in 1995; it provides a 10 fiber ribbon between transmitter and receiver arrays, with an aggregate data rate of 2.4 Gbit/s over 300 m. Since then, there have been many vendors who have demonstrated prototype POIs (3). Although there is not yet a common standard for these devices, most are based on short wavelength VCSELs and are limited to a few tens or hundreds of meters. There is no standardization on the ribbon connectors; although many products are based on the MTP/MPO 12 fiber ferrule, different manufacturers have developed at least a half dozen proprietary implementations which are not compatible. Applications for POI include highly parallel supercomputers or clustered multiprocessors for large servers, large telecom or datacom switches, channel extensions for existing parallel data buses such as the Small Computer Interface (SCI), and options for emerging parallel bus standards such as HIPPI 6400. Research into VCSELs capable of operating at longer wavelengths (1300 nm) promise to extend the distance of future parallel optical interconnects; development of two-dimensional arrays and so-called smart pixel technology are also very promising areas of future research.

Plastic Fiber

The first research in optical fiber transmission was conducted around 1955 using crude plastic fibers. There has been recent research into the use of large-core plastic fiber as a low-cost optical data link. Because of the much higher volumes of glass fiber manufactured today, the cost of plastic optical fiber remains higher than glass in the short term. Plastic fibers are currently limited by their high loss (120 dB/km to 150 dB/km) to fairly short distances (around 50 to 100 m). The bandwidth at 100 m is approximately 125 MHz. Despite this, there is ongoing interest in this technology because plastic fiber links can use very-low-cost visible light sources; a 680 nm (red) LED transceiver could be as inexpensive as \$5 to \$10, compared with over \$100 for a 1300 nm transceiver. Plastic fiber links have already found some applications in laser printers and microprocessor control systems for automobiles. Fusion splices in plastic fiber exhibit very high loss, approximately 5 dB. Several plastic fiber connectors have been proposed, including variations on the F07, SMA 905 and 906, EIAJ Digital Audio, ST, and FC connectors. Step index plastic fiber has a core diameter of 980 μm and a 20 μm cladding, over 100 times larger than singlemode fiber; its NA is approximately 0.3. The most common material used today is called for poly(methyl methylacrylate) (PMMA). While the attenuation of plastic fiber remains higher than glass, transmission with visible sources at 570 nm and 650 nm is feasible.

Another type of specialty fiber is hard polymer clad fiber (HPCF), which is a glass fiber with a hard plastic cladding. It attempts to combine the advantage of glass and plastic fiber while overcoming some of their drawbacks. Typical HPCF fiber has a core diameter of 200 μm, cladding diameter of 225 μm, attenuation of 0.8 dB/100 m, NA of 0.3, and bandwidth of 10 Mhz/km. If we use visible wavelengths of approximately 650 nm, attenuation is relativly high; all HPCF is step index only. The attenuation of HPCF fiber is shown in Fig. 19.

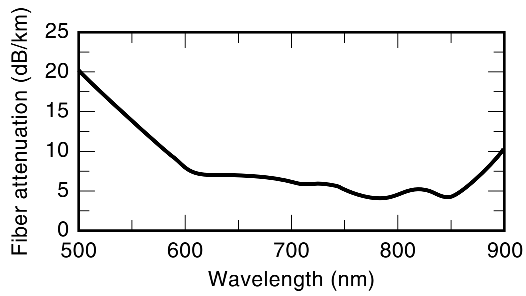

Figure 19. Attenuation of HPCF optical fiber plotted against wavelength.

Wavelength Multiplexing

Optical wavelength division multiplexing (WDM) is a way to take advantage of the high bandwidth of fiber optic cables without requiring extremely high modulation rates at the transceiver. Because different wavelengths do not interfere with each other, multiple datastreams may be combined in a single optical fiber. Coarse WDM schemes utilize only a few wavelengths spaced far apart; some systems use only two signals at 1300 nm and 1550 nm. More complex dense WDM systems may employ tens of wavelengths spaced apart 1 nm or less, typically in the region of minimal dispersion close to 1550 nm. Such systems require that the wavelength of the optical transmitter be held very stable, often incorporating temperature and voltage control of the source. The optical signals at different wavelengths may be combined using passive optical components such as splitters, couplers, prisms, or diffraction gratings. For systems with a small number of channels, phase array multiplexers are preferred; they consist of an array of dispersive waveguides with variable pathlengths that can be used to focus light from an input port to a number of different output ports depending on the wavelength of the light. It is also possible to employ sources that are wavelength tunable; examples include external cavity lasers with a frequency selective component such as a filter or diffraction grating. Two- or three-section distributed feedback lasers may also be tuned over a narrow wavelength range by varying an applied electric current (57). When the optical signals are demultiplexed, they must be separated at the optical receiver; this can be done using filters or by means of tunable receivers that select the desired wavelength in response to an applied electric current. The simplest form of a tunable receiver is a single cavity Fabry–Perot interferometer with a movable mirror that creates a tunable resonant cavity. Cascaded Mach–Zender interferometers with variable phase delay in one branch may also be used. Switchable gratings such as the monolithic grating spectrometer or acousto-optic tunable filter may also be employed. There is ongoing research in the area of all-optical networks incorporating these components. One possible network architecture is the broadcast-and-select network (3), which consists of nodes interconnected via a star coupler. Optical fiber carries signals from each node to the star, where they are combined and distributed to all other nodes equally; examples include the Lambda (3) and Rainbow (3) networks. A wavelength-routed network consists of either static or reconfigurable wavelength selective routers interconnected by fiber links. Currently there are no standards for WDM networking, although the International Telecommunications Union is developing a draft standard G.692 entitled "Optical interfaces for multichannel systems using optical amplifiers."

Solitons

Next to attenuation, dispersion is the most important factor in determining the ultimate length of an optical link. Solitons have received strong interest in the optical communications area because they represent a solution to the wave equation (a hyperbolic secant pulse shape) which propagates without dispersion on standard optical fiber. This is achieved by balancing two effects: self-phase modulation and chromatic dispersion (also known as group velocity dispersion) in the fiber. Self-phase modulation is caused when optical pulses have sufficiently high intensity to modify the refractive index of the fiber via the nonlinear Kerr effect. This causes a chirp in the optical signal such that longer wavelengths move toward the beginning of the optical pulse and shorter wavelengths to the end. In standard optical fiber at wavelengths greater than 1310 nm (the so-called anomalous dispersion regime), chromatic dispersion causes shorter wavelengths to travel faster than longer ones, such that shorter wavelengths tend to move toward the beginning of the pulse (the opposite direction from self-phase modulation). Thus, if these two effects exactly balance each other, the pulse shape is retained during propagation; of course, pulses still suffer attenuation and must be periodically amplified. The effect only occurs at wavelengths greater than 1310 nm, for which the group velocity dispersion in standard fiber is negative; otherwise, the pulses would suffer increased dispersion. This raises the possibility of optical communication over very long distances, and at very high data rates when combined with time division multiplexing techniques.

Related areas of research include dark soliton; a small gap within an unbroken, high power optical beam or a very long pulse will behave exactly like a regular soliton. It is also possible for the soliton effect to be spatial rather than temporal; high-power optical beams can be used to modify the refractive index of dispersive media in such a way that they create their own waveguides. Such spatial solitons remain localized in space as if they were confined in a waveguide by balancing the effects of diffraction (spatial dispersion) and self-phase modulation.

Optical Amplifiers

An optical amplifier is a device that amplifies the optical signal directly without ever converting it into an electrical signal. This makes the signal amplification independent of the type of data encoding used, since retiming of the signal is not required as in a digital regenerator. There are many possible types of optical amplifiers. Almost any semiconductor laser can be converted into an amplifier by increasing the length of the gain region; such devices are called semiconductor optical amplifiers, and are most useful at wavelengths near 1300 nm. In the late 1980s, researchers developed fiber-based amplifiers, which amplify optical signals by passing them through a specially doped length of fiber (approximately 10 m) which couples light from a separate optical pump source into the desired optical signal. The fibers are typically doped with rare earth elements such as erbium, neodynium, or praseodymium, and operate on the same principle as a laser. Rare earth ions are pumped into elevated energy states by using a relatively high-powered optical source (10 mW to 200 mW) at a different wavelength than the desired signal (980 nm or 1400 nm optical pumps are most common). A photon from the desired signal will then cause stimulated emission at the same wavelength as the desired signal (1300 nm or 1550 nm). In this way, a band of wavelengths approximately 24 nm wide can be optically amplified. Reflections back into the amplifier from the attached fiber must be controlled using optical isolators to insure stable operation of the amplifier. Erbium-doped amplifiers operating near 1550 nm are most commonly in use today; they offer low insertion loss, low noise, and minimal interchannel crosstalk and polarization sensitivity. The gain characteristic of a typical erbium-doped optical amplifier is shown in Fig. 20 (note the logarithmic scale). The gain is not uniform over the passband; it is approximately 3 dB higher at 1560 nm than at 1540 nm. If several amplifiers are cascaded in series, this effect is cumulative and results in significant nonuniform amplification at different wavelengths. A further complication is that the gain profile changes with signal power levels, so that the amplifier response will be different depending on the number of channels being amplified at once in a WDM system. Most optical amplifiers operate in gain saturation or beyond the point where further increase in the input power does not result in a corresponding increase in output power (in this respect, optical amplifiers behave very differently from electrical amplifiers, which are subject to nonlinear distortion when they saturate). This is possible because erbium amplifiers respond to changes in average power (fluctuations over the course of a few milliseconds) rather than to instantaneous changes in power levels as for electrical amplifiers. Current research is directed toward flattening the gain curve; this can be done in many ways, for example by introducing other dopants including aluminum or ytterbium, controlling the pump power through a feedback loop, gain clamping (addition of an extra WDM channel locally at the amplifier to absorb excess power), or incorporating preemphasis filters and blazed diffraction gratings into the system. These amplifiers also suffer from amplified spontaneous emission noise and significant broadening of the amplified signal spectra; secondary effects such as stimulated Raman scattering must also be controlled at the system level.

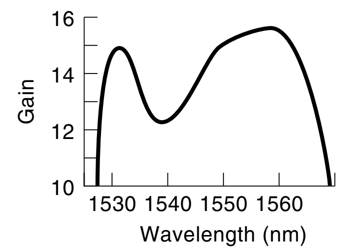

Figure 20. Gain curve of a typical erbium doped fiber amplifier.

CONCLUSION

Since the technology for optical communications over fiber first emerged in the 1970s, the need for higher bandwidth, faster speed, and longer distances has driven a host of new applications. This area is experiencing rapid growth, however, estimated by some to be as much as 25% compounded annually through the turn of the century. As of this writing, there is enough fiber installed in the world today to stretch between the earth and the moon 28 times. The past decade has seen a reduction in the size and cost of optical transceivers comparable to the transition from vaccum tubes to solid-state semiconductor chips in the electronics industry. As fiber optic technology continues to evolve, several trends have emerged; the use of smaller form factors and nonhermetic transceiver packaging, transceivers that operate at lower voltages to dissipate less power, advances in optoelectronic packaging including plastic housings, sleeves, fiber, and ferrules, and growing interest in WDM, optical amplifiers, and parallel optics as ways to increase the available bandwidth of a communication link.

Predicting the future of optical communications is a proposition fraught with uncertainty. As the datacom industry has continued to evolve, many people have tried to speculate what the future will bring. In 1965, Gordon Moore (founder and current chairman of Intel Corporation) projected that computing power as measured by the logic density of silicon integrated circuits would grow exponentially, roughly doubling every 12 months to 18 months (3). This has held true for the past 30 years, and has come to be known as Moore's Law. Recent presentations by Moore (3) forecast that this trend will continue through the next decade or so, as feature sizes approach 0.18 μm and as the economic problems associated with fabricating such chips begin to be felt. Observing that the usefulness of this computer power depends on the number of networked users, in 1980 Bob Metcalfe argued that the value of a network can be measured by the square of the number of users (3). Metcalfe's Law is more fully described by George Gilder, also the namesake for the Gilder Paradigm (3), which predicts in part that future communication system designs will be influenced by a key scarcity of bandwidth. In this same spirit, similar predictions can be made concerning the growth of bandwidth requirements in data communications following the recent introducton of fiber optics (before the widespread use of fiber, data rates appear to have increased only incrementally over a relatively long period of time). During a recent technical conference (1996 Optical Society of America Annual Meeting), for example, the author introduced a graph showing the extrapolated growth of input–output bandwidth on mainframes and large servers as a measure of leading-edge application requirements. This bandwidth has been growing exponentially since about 1988, when optical fiber first became available as an option on the IBM System/390. This trend, labeled by one of the meeting attendees as DeCusatis' Law, is projected to continue for at least the next several generations of CMOS-based large mainframe computer systems, and perhaps beyond.

BIBLIOGRAPHY

1. S. E. Miller and A. G. Chynoweth (eds.), *Optical Fiber Telecommunications,* New York: Academic Press, 1979.
2. J. Gowar, *Optical Communication Systems,* Englewood Cliffs, NJ: Prentice-Hall, 1984.
3. C. DeCusatis et al. (eds.), *Handbook of Fiber Optic Data Communication,* New York: Academic Press, 1998.
4. R. Lasky, U. Osterberg, and D. Stigliani (eds.), *Optoelectronics for Data Communication,* New York: Academic Press, 1995.
5. J. Senior, *Optical Fibre Communications: Principles and Practice,* 2nd ed., Englewood Cliffs, NJ: Prentice-Hall, 1982.
6. P. Green, *Fiber Optic Networks,* Englewood Cliffs, NJ: Prentice-Hall, 1993.
7. J. Laude, *Wavelength Division Multiplexing,* Englewood Cliffs, NJ: Prentice-Hall, 1993.
8. United States laser safety standards are regulated by the Dept. of Health and Human Services (DHHS), Occupational Safety and Health Administration (OSHA), Food and Drug Administration (FDA), Code of Radiological Health (CDRH), 21 Code of Federal Regulations (CFR) subchapter J; the relevant standards are ANSI Z136.1, *Standard for the Safe Use of Lasers* (1993 revision) and ANSI Z136.2, *Standard for the Safe Use of Optical Fiber Communication Systems Utilizing Laser Diodes and LED Sources* (1996–97 revision); elsewhere in the world, the relevant standard is International Electrotechnical Commission (IEC/CEI) 825 (1993 revision).
9. Electronics Industry Association/Telecommunications Industry Association (EIA/TIA) commercial building telecommunications cabling standard (EIA/TIA-568-A). Detail specification for 62.5 μm core diameter/125 μm cladding diameter class 1a multimode graded index optical waveguide fibers (EIA/TIA-492AAAA), detail specification for class IV-a dispersion unshifted single-mode optical waveguide fibers used in communication s systems (EIA/TIA-492BAAA) Electronics Industry Association, New York.
10. J. P. Powers, *An Introduction to Fiber Optic Systems,* Homewood, IL: Aksen, 1993.
11. D. Marcuse, D. Gloge, and E. A. J. Marcatiti, Guiding properties of fibers, in *Optical Fiber Telecommunications,* S. E. Miller and A. G. Chynoweth (eds.), New York: Academic Press, 1979.
12. D. Marcuse, Loss analysis of single mode fiber splices, *Bell System Tech. J.,* **56**: 703–718, 1977.
13. T. Okoshi, *Optical Fibers,* New York: Academic Press, 1982.
14. P. K. Cheo, *Fiber Optics and Optoelectronics,* 2nd ed., Englewood Cliffs, NJ: Prentice-Hall, 1990.
15. S. Nemoto and T. Makimoto, Analysis of splice loss in single-mode fibers using a Gaussian field approximation, *Opt. Quantum Electron.,* **11**: 447–457, 1979.
16. J. R. Webb and U. L. Osterberg, Fiber, cable, and coupling, in R. Lasky, U. Osterberg, and D. Stigliani (eds.), *Optoelectronics for Data Communication,* New York: Academic Press, 1995.
17. E. G. Neumann, *Singlemode Fibers: Fundamentals,* Berlin: Springer-Verlag, 1988.
18. S. S. Walker, Rapid modeling and estimation of total spectral loss in optical fibers, *IEEE J. Lightwave Technol.,* **4**: 1125–1132, 1996.
19. D. Gloge, Propagation effects in optical fibers, *IEEE Trans. Microwave Theory Tech.,* **MTT-23**: 106–120, 1975.
20. P. M. Shanker, Effect of modal noise on single-mode fiber optic network, *Opt. Commun.,* **64**: 347–350, 1988.
21. C. DeCusatis and M. Benedict, Method for fabrication of high bandwidth optical fiber, *IBM Tech. Disc. Bulletin,* May 1992.
22. J. J. Refi, LED bandwidth of multimode fiber as a function of source bandwidth and LED spectral characteristics, *IEEE J. Lightwave Technol.,* **LT-14**: 265–272, 1986.
23. S. E. Miller and I. P. Kaminow (eds.), *Optical Fiber Telecommunications II,* New York: Academic Press, 1988.
24. G. P. Agrawal et al., Dispersion penalty for 1.3 micron lightwave systems with multimode semiconductor lasers, *IEEE J. Lightwave Technol.,* **LT-6**: 620–625, 1988.

25. K. Ogawa, Analysis of mode partition noise in laser transmission systems, *IEEE J. Quantum Electron.,* **QE-18**: 849–9855, 1982.
26. K. Ogawa, Semiconductor laser noise; mode partition noise, in R. K. Willardson and A. C. Beer (eds.), *Semiconductors and Semimetals,* Vol. 22C, New York: Academic Press, 1985.
27. J. C. Campbell, Calculation of the dispersion penalty of the route design of single-mode systems, *IEEE J. Lightwave Technol.,* **LT-6**: 564–573, 1988.
28. M. Ohtsu et al., Mode stability analysis of nearly single-mode semiconductor laser, *IEEE J. Quantum Electron.,* **GE-24**: 716–723, 1988.
29. M. Ohtsu and Y. Teramachi, Analysis of mode partition and mode hopping in semiconductor lasers, *IEEE J. Quantum Electron.,* **25**: 31–38, 1989.
30. D. Duff et al., Measurements and simulation of multipath interference for 1.7 Gbit/s lightwave systems utilizing single and multifrequency lasers, *Proc. Optical Fiber Conf., San Diego, CA,* 1989, p. 128.
31. J. Radcliff, *Fiber Optic Link Performance in the Presence of Internal Noise Sources,* IBM Tech. Rep., Glendale Labs, Endicott, NY, 1989.
32. L. L. Xiao, C. B. Su, and R. B. Lauer, Increase in laser RIN due to asymmetric nonlinear gain, fiber dispersion, and modulation, *IEEE Photon. Technol. Lett.,* **PTL-4**: 774–777, 1992.
33. CCITT, Geneva, Switzerland, *Recommendations G.824, G.823, O.171, and G.703 on Timing Jitter in Digital Systems,* 1984.
34. A. A. Manalino, Time domain eyewidth measurements of an optical data link operating at 200 Mbit/s, *IEEE Trans. Instrum. Meas.,* **IM-36**, 551–553, 1987.
35. F. M. Gardner, *Phaselock Techniques,* 2nd ed., New York: Wiley, 1979.
36. G. P. Agrawal and T. P. Shen, Power penalty due to decision time jitter in optical communication systems, *Electron. Lett.,* **22**: 450–451, 1986.
37. T. M. Shen, Power penalty due to decision time jitter in receiver avalanche photodiodes, *Electron. Lett.,* **22**: 1043–1045, 1986.
38. P. R. Trischitta and E. L. Varma, *Jitter in Digital Transmission Systems,* Boston: Artech House, 1989.
39. C. J. Byrne, B. J. Karafin, and D. B. Robinson Jr., Systematic jitter in a chain of digital regenerators, *Bell Syst. Tech. J.,* **43**: 2679–2714, 1963.
40. R. J. S. Bates and L. A. Sauer, Jitter accumulation in token passing ring LANs, *IBM J. Res. Develop.,* **29**: 580–587, 1985.
41. C. Chazmas, Accumulation of jitter, a stochastic model, *AT&T Tech. J.,* **64**: 120–134, 1985.
42. P. M. Shanker, Effect of modal noise on single-mode fiber optic networks, *Opt. Commun.,* **64**: 347–350, 1988.
43. J. B. Haber et al., Assessment of radiation induced loss for AT&T fiber optic transmission systems in the terrestrial environment, *IEEE J. Lightwave Technol.,* **6**: 150–154, 1988.
44. M. Kyoto et al., Gamma ray radiation hardened properties of pure silica core single-mode fiber and its data link system in radioactive environments, *IEEE J. Lightwave Technol.,* **10**: 289–294, 1992.
45. D. Cotter, Observation of stimulated Brillouin scattering in low loss silica fibers at 1.3 microns, *Electron. Lett.,* **18**: 105–106, 1982.
46. H. J. A. diSilva and J. J. O'Reily, System performance implications of laser chirp for long haul high bit rate direct detection optical fiber systems, *Proc. IEEE Globecom.,* 1989, pp. 19.5.1–19.5.5.
47. R. H. Stolen and C. Lin, Self-phase modulation in silicon optical fiber, *Phys. Rev. A,* **17**: 1448, 1978.
48. D. Stigliani, Enterprise systems connection fiber optic link, in C. DeCusatis et al. (eds.), *Handbook of Optoelectronics for Fiber Optic Data Communications,* New York: Academic Press, 1998.
49. *ESCON I/O Interface Physical Layer Document,* 3rd ed. (IBM document number SA23-0394), Mechanicsburg, PA: IBM Corporation, 1995.
50. *ANSI Single Byte Command Code Sets CONnection architecture (SBCON),* draft ANSI standard X3T11/95-469 (rev. 2.2), 1996, available from Global Engineering Documents, Santa Ana, CA.
51. ANSI X3.230-1994 rev. 4.3, *Fibre Channel—Physical and Signaling Interface* (FC-PH), ANSI X3.272-199x, rev. 4.5, *Fibre Channel—Arbitrated Loop* (FC-AL), June 1995, ANSI X3.269-199x, rev. 012, *Fibre Channel Protocol for SCSI (FCP),* May 30, 1995.
52. ANSI T1.105-1988, *Digital Hierarchy Optical Rates and Format Specification,* 1988, available from Global Engineering Documents, Santa Ana, CA.
53. CCITT Recommendation G.707, *Synchronous Digital Hierarchy Bit Rates,* 1988, available from International Telecommunications Union, Geneva, Switzerland.
54. CCITT Recommendation G.708, *Network Node Interfaces for the Synchronous Digital Hierarchy,* 1988, available from International Telecommunications Union, Geneva, Switzerland.
55. CCITT Recommendation G.709, *Synchronous Multiplexing Structure,* 1988, available from International Telecommunications Union, Geneva, Switzerland.
56. IEEE 802.3z, *Draft Supplement to Carrier Sense Multiple Access with Collision Detection (CSMA/CD) Access Method and Physical Layer Specifications: Media Access Control (MAC) Parameters, Physical Layer, Repeater and Management Parameters for 1000 Mb/s Operation,* June 1997, available from Institute of Electrical and Electronics Engineers, Piscataway, NJ.
57. H. Dutton, *Optical Communication Technology: An Introduction and Tutorial,* New York: Academic Press, 1998.

CASIMER DECUSATIS
IBM Corporation

OPTICAL COMMUNICATION EQUIPMENT. See DEMULTIPLEXING EQUIPMENT.

OPTICAL COMPONENTS. See PACKAGING OF OPTICAL COMPONENTS AND SYSTEMS.

OPTICAL CONSTANTS. See OPTICAL PROPERTIES.

OPTICAL CORRELATION. See MATCHED FILTERS.

OPTICAL DATA LINK PACKAGING. See PACKAGING OF OPTICAL COMPONENTS AND SYSTEMS.

OPTICAL FIBERS, ATTENUATOR. See ATTENUATION MEASUREMENT.